Contents lists available at ScienceDirect

Palaeogeography, Palaeoclimatology, Palaeoecology

journal homepage: www.elsevier.com

Post-mortem alteration of diet-related enamel surface textures through artificial biostratinomy: A tumbling experiment using mammal teeth

Katrin Böhm[a,*], Daniela E. Winkler[a], Thomas M. Kaiser[b], Thomas Tütken[a]

[a] Applied and Analytical Palaeontology, Institute of Geosciences, Johannes Gutenberg University, J.-J.-Becher-Weg 21, 55128 Mainz, Germany
[b] Center of Natural History (CeNak), University of Hamburg, Germany

ARTICLE INFO

Keywords:
Dental wear
Surface texture
Microwear
Diagenetic alteration
Biostratinomy
Mammal teeth

ABSTRACT

In the fossil record, teeth are often all that remains of a fossil organism. Dental microwear texture analysis (DMTA) is a common proxy for diet using dental wear features at the μm-scale, enabling comparative and quantitative assessments of various feeding traits in extant and extinct species. In extinct species, original diet-related dental wear features may be overprinted by post-mortem alteration including fluvial transport. Here we experimentally investigate the effects of mechanical alteration on diet-related 3D enamel surface texture (3DST) patterns of different mammal teeth. Post canine teeth of *Equus* sp., *Capreolus capreolus* and *Otomys* sp. are tumbled in sediment-water suspensions using three different grain size fractions of sand. The 3DST of the enamel surfaces are measured prior to and after each tumbling interval and characterised using ISO normed surface texture and SSFA parameters. In all species, we find several parameters to be almost unaffected by tumbling (stable parameters), while other parameters show inconsistent-directional shifts (unstable parameters). For *Otomys*, all three sediment grain size fractions result in abrasion of peaks and a reduction of overall surface roughness. For *Equus*, tumbling results in visible abrasive changes in the original wear patterns and the introduction of new wear features. *Capreolus capreolus* shows high variability in surface texture patterns prior to and after the experiment, hence we see ambiguous trends for changes in parameter values. However, even after 336 h of tumbling the browsing *C. capreolus* can still be distinguished from the grazing *Equus* sp.

Thus, biostratinomy may potentially modify diet-related 3DST causing non-systematic bias via mechanical abrasion, which is related to sediment grain size, duration of transport and geometry of teeth. However, the original diet-related 3DST is still preserved and a more prominent characteristic in DMT than the experimentally induced diagenetic alteration.

1. Introduction

Dental microwear texture analysis (DMTA) is a powerful proxy for oral behaviour, reflecting the mechanical properties of ingesta consumed during the last few days or weeks, and for tooth function in general. The tribosystem of occluding teeth is largely controlled by abrasion and attrition as a cause of material loss (Dahlberg and Kinzey, 1962). Patterns of wear features at μm-scales (roughness texture) can be related to feeding traits, enabling quantitative and comparative assessments of diet/ingesta related traits such as soft- or hard-object feeding among extant and fossil vertebrates (Solounias et al., 1988; Scott et al., 2005; Merceron et al., 2007; Semprebon and Rivals, 2007; Schulz et al., 2010; Winkler et al., 2013). Baker et al. (1959) were among the first to link microscopic wear features on teeth with abrasives ingested in the diet. In their study of sheep teeth, they concluded that internal abrasives, such as phytoliths, where hard enough to scratch enamel and thus indicate diet. Since then, many studies of tooth wear analyses at different spatial scales (mesowear, microwear, dental microwear texture analysis) for a large variety of vertebrates (mostly mammals) have been performed, and characteristic wear patterns related to their assumed natural diets have been described (Fortelius and Solounias, 2000; Schulz et al., 2010; Fraser and Theodor, 2011; DeSantis et al., 2013; Purnell et al., 2013; Calandra and Merceron, 2016).

In the fossil record, teeth are often the only preserved parts of animals and are therefore a crucial source of information about the feed-

* Corresponding author.
Email addresses: kboehm@students.uni-mainz.de (K. Böhm); daniela.winkler@uni-mainz.de (D.E. Winkler); thomas.kaiser@uni-hamburg.de (T.M. Kaiser); tuetken@uni-mainz.de (T. Tütken)

https://doi.org/10.1016/j.palaeo.2019.01.008
Received 4 June 2018; Received in revised form 13 October 2018; Accepted 4 January 2019
Available online xxx
0031-0182/ © 2019.

UNCORRECTED PROOF

ing behaviour of extinct taxa. Dietary reconstructions based on the wear features of fossil occlusal tooth surfaces can easily be biased post-mortem due to mechanical and/or chemical modification (King et al., 1999; Dauphin et al., 2018). Therefore, reconstructions should be restricted to areas of a tooth which are relatively unaltered by post-mortem processes. This makes distinguishing between ante- and post-mortem surface alterations a crucial issue for reliable palaeodietary reconstructions based on 3DST (Calandra and Merceron, 2016).

There are two primary sources of post-mortem mechanical surface alteration on teeth (Teaford, 1988):

1. Material loss occurring after death or before/during the burial of an animals remains.
2. Material loss caused by excavation and preparation during/after the collection of a fossil.

Both sources of mechanical surface alteration can have an impact on ante-mortem occlusal wear features and possibly alter or obscure those wear features. Most post-mortem wear features are distinctively different in their size, shape or orientation (Teaford, 1988). In addition to mechanical alteration, chemical alteration may modify ante-mortem wear features, e.g. by acid attack in the stomach of a predator (e.g. Dauphin et al., 2003, 2018) or by dissolution processes in the soil/sediment environment. Overall, there is a substantial lack of experimental data on the effect of biostratinomy on mammalian teeth. Gordon (1983, 1984) tumbled extracted human molars and premolars with four different types of sediment, ranging from volcanic ash to "pea" gravel (~4–8 mm), in aqueous and non-aqueous environments for different time intervals (unspecified). Gordon found significant changes to the ante-mortem dental wear after 5 h and determined that alteration of the microwear pattern correlated positively with sediment grain size. However, tumbling seemed to abrade the identifiable microwear rather than add or produce new wear features (Gordon, 1984). Similarly, King et al. (1999) tumbled three human lower molar teeth from the late Neolithic with three different grain size fractions of sediment and water for 2–512 h and found evidence for changes in dental microwear only with the smallest grain size fraction. Coarse sand (500–1000 μm) produced no change in dental microwear and quartz pebbles (2000–11,000 μm) also resulted in little surface damage on the tooth. However, a noticeable abrasive effect was observed for the grain size fraction between 250 and 500 μm, which completely removed the original microwear features. Both studies showed a polishing effect on the dental surface rather than formation of new wear features comparable in morphology with those of the ante-mortem wear (Gordon, 1984; King et al., 1999). Nevertheless, taphonomically altered dental wear patterns could still be easily identified and distinguished from diet-related wear patterns (Teaford, 1988; King et al., 1999). For example, Martínez and Pérez-Pérez (2004) tested whether taphonomic and non-taphonomic wear features were clearly distinguishable on the buccal enamel surfaces of fossil hominin teeth from Olduvai and Laetoli (Martínez and Pérez-Pérez, 2004). In this sample, they found evidence for both chemical and mechanical alteration, as well as for well-preserved dental surface areas with no obvious post-mortem material loss, enabling the identification of taphonomically altered teeth. The combination of mechanical and chemical post-mortem wear has often drastically reduced sample sizes of analyses of fossil material (e.g., Ungar et al., 2008), however, this may not always be necessary.

All experimental studies conducted thus far are qualitative and have only been performed on human teeth. Although there are numerous studies connecting dental wear in other mammalian taxa with ingesta properties (i.e. Mainland, 2003a, 2003b), there is as of yet no experimental approach to assess the influence of post-mortem abrasion on non-human teeth. Here we present the first experiment to quantitatively test the effect of biostratinomy on DMTA in three different herbivorous mammalian species.

We employ an experimental setup with three different sediment grain size fractions (fine to middle sand, 63–500 μm) and different tumbling time periods (from 0.5 to 336 h). Dental surface texture measurements of the same areas on wear facets were performed on teeth of three herbivorous (grazer and browser) mammals (*Otomys* sp., *Capreolus capreolus* and *Equus* sp.) before and after each tumbling interval, using a high-resolution disc-scanning confocal 3D-surface measuring system μsurf Custom. To quantify dental wear and detect potential alteration by the selected sediments during the experiments, two DMTA methods were employed: scale-sensitive fractal analysis (SSFA) and, what we refer to as 3D surface texture analysis (3DST). Both approaches employ optical profilometry to obtain 3D representations of the enamel surface at submicron resolution and evaluate the overall distribution and three-dimensional geometry of topographic features. In SSFA, surface features are characterised using length-scale and area-scale fractal analyses, describing complexity and anisotropy of the surface (e.g. Ungar et al., 2003, 2012; Scott et al., 2006; Scott, 2012). In 3DST, standardised roughness (ISO 25178) and flatness (ISO 12781) parameters plus additional motif, furrow, direction and parameters are employed to characterise wear features (Schulz et al., 2013a, 2013b; Purnell and Darras, 2016; Kubo et al., 2017; Purnell et al., 2017). A major focus of diet reconstruction via dental wear has been on the browser-grazer dichotomy in the artiodactyla and perissodactyla (e.g. Rensberger, 1973; Fortelius and Solounias, 2000; Damuth and Janis, 2011; Fraser and Theodor, 2011; Schulz et al., 2013a). The browser-grazer dichotomy is well reflected at the different scales of dental wear evaluation (i.e. mesowear, microwear, and dental microwear texture analysis). Browsers are characterised by less abraded tooth wear, which is reflected in a mesowear profile with sharp cusps (Fortelius and Solounias, 2000; Kaiser et al., 2000). The surface is dominated by high complexity and low anisotropy values (SSFA, Scott, 2012; Ungar et al., 2012) and an overall smooth surface with low microscopic peaks (3DST, Schulz et al., 2013a, 2013b) and pits (microwear, Walker et al., 1978). In contrast, grazers show mesowear dominated by rounded or blunt cusps and scratches (microwear, Walker et al., 1978), with an overall greater surface roughness, higher and more frequent peaks and deeper dales but a generally less variable pattern (3DST, Schulz et al., 2013a, 2013b) and high anisotropy/low complexity values (SSFA, Scott, 2012; Ungar et al., 2012).

The aim of this study is to test whether diet-related 3DST (i.e. browser-grazer differences) are resistant against mechanical alteration during sediment transport under a post-mortem abrasive regime. If biostratinomical changes on the wear facets of teeth occur, are they recognizable as post-mortem wear or do they show patterns comparable to ante-mortem wear? We therefore tested if the 3DST of teeth from a grazer (*Equus* sp.) and browser (*Capreolus capreolus*) could still be assigned to the correct dietary category after tumbling intervals of up to 336 h. In other words, could the surface texture parameters normally found to distinguish between these two dietary categories still distinguish between browsers and grazers despite mechanical abrasion meant to mimic sediment transport? We expect that different surface texture parameters will be affected differently by our experimental setup. We anticipate that parameters which describe extremes of the surface (e.g. maximum height) will more prone to alteration by abrasion compared to parameters describe mean roughness of the surface. Thus, we intend to identify parameters that show the potential to bias dietary interpretations. Our goal is further to not only test the hypothesis that sediment grain size has an impact on dental microwear texture, but that tooth geometry does as well. Additionally, we analysed the altered parameters after the experiment to test whether the extreme outliers in parameter values can be used as indicators of taphonomic alteration.

UNCORRECTED PROOF

2. Material and methods

Cheek teeth from three different extant small and large mammal taxa were used to investigate the physical effects of post-mortem abrasive action on 3DST patterns on chewing facets. Due to the potentially destructive nature of the experiment, dental material with low scientific value (e.g. no precise locality data) was used. This resulted in a variable sample composition including both molars and premolars and, due to unequal preservation, different enamel facets (Fig. 1). Such a sample composition is thus more representative of the type of mixed tooth assemblage often recovered in the fossil record.

Nine teeth of each taxon were used: molars and premolars belonging to *Equus* sp. (zebra), *Otomys* sp. (African vlei rat or groove-toothed rat) and *Capreolus capreolus* (roe deer) (Table 1). The samples represent wild species from landscape and museum collections, with no obvious sign of post-mortem dental alteration. The zebra teeth have a mean occlusal width of 2–3 cm, the roe deer 1.5–2 cm. The *Otomys* teeth are the smallest with ~ 2–4 mm in length (Fig. 1). Zebra and roe deer samples have the same prismatic structure in mature enamel, with horizontally arranged multiserial Hunter-Schreger bands (Hillson, 2005). Rodent molar teeth have enamel with a more irregular and less sharply defined structure on the occlusal surface (Hillson, 2005). All specimens were tumbled in sediment-water suspensions containing siliciclastic sediment particles of three different grain sizes (63–125 μm, 125–250 μm and 250–500 μm) using commercially available tumbling machines. For each grain size fraction, three teeth of each species (one per barrel) were tumbled for eight different time intervals of 0.5, 1, 2, 4, 8, 12, 16 and 336 h (Table 1). At each 3DST measurement, the tumbling interval was interrupted and continued after the measurement.

2.1. Sample preparation

The teeth were cleaned manually using cotton swabs and water to remove adhering dust, ethanol to remove lipids and acetone to remove any residual acetone-soluble varnishes/superglue. 3DST measurements were taken of the original ante-mortem occlusal texture according to the protocol of Schulz et al. (2013a) for all dental specimens except for three molars of *Capreolus capreolus,* in which the high cusps and steeply inclined wear facets did not allow for direct measurements on the original teeth. For these *C. capreolus* specimens, moulds of the facet surface of each of the three molars were produced using high-resolution silicone-Vinylpolysiloxane precision impression material Provil novo Light regular set EN ISO 4823, type 3, light (Heraeus Kulzer GmbH, Dormagen, Germany).

Two cutmarks were placed on the target facets of the *Equus* sp. and *C. capreolus* (pre-)molars (facets 1–4, Fig. 2) in order to define a measurement area. Four non-overlapping scans of 160 × 160 μm were taken on all suitable and marked wear facets (Fig. 1). In order to identify and measure the same areas on the occlusal surface after each tumbling interval, the wear facet was optically aligned to the referring cutmark and measured at the same relative coordinates as in the previous measurements. Since there were possible inaccuracies during the orientation of the teeth at each measuring interval, a rotation of the wear facet around 5–10° was accepted. *Otomys* teeth were too small and delicate to use cutmarks, however, the small size and number of enamel lamellae enabled precise re-identification of focal measurement positions. (Fig. 2, Table 1). Four non-overlapping scans were measured per tooth.

2.2. Sediment

Construction grade joint-sand (Flairstone) was sieved using DIN norm sieves (500 μm, 250 μm, 125 μm and 63 μm), into three different grain size fractions: 63–125 μm, 125–250 μm, 250–500 μm. Based on grain size analysis with laser granulometry, the true grain size fractions have a median of 101 μm (range: 51–168 μm), 200 μm (range: 112–292 μm) and 353 μm (221–513 μm) (Fig. 3). The grain size fractions thus overlap somewhat, potentially due to aggregate formation and disintegration; nevertheless, the median fits the considered grain size fractions. In the following, the grain size fractions are labelled as follows: very fine sand (51–168 μm), fine sand (112–292 μm) and medium sand (221–513 μm). Based on X-ray diffraction measurements, quartz is the principle mineral phase in all three sand fractions. In the fine sand, the quartz content is slightly higher (~60%) than in the other two grain size fractions (~50–55%). Additionally, feldspar (albite) is a component of the sediment in all three sand fractions.

2.3. Tumbling procedure

The effects of fluvial transport in a suspension of sediment particles were simulated using commercial hobby rotary tumblers TYP TRO 2 A (Otto Eigner e.K., Industriebedarf & Hobbyschleifmaschinen, Idar-Oberstein, Germany). Tumbling barrels have a diameter of 10 cm and a capacity of 900 ml. Machines operate at a constant speed of 45 rpm, which equals a transport speed of around 1.08 km per hour. As comparison, the Rhine river flows with a speed of around 2.5–10.5 km per h (Wasserstraßen-und Schifffahrstverwaltung des Bundes). In order to ensure a constant suspension of sediment in water during tumbling and to facilitate contact between the tooth and sediment, the barrels were filled with 500 g of sediment and 300 ml of tap water (resulting in a 90% full barrel). For each barrel, one tooth was added to the sediment-water mixture and each tooth was then tumbled for 0.5, 1, 2, 4, 8, 12 and 16 h (Table 1). These time intervals were chosen to represent the

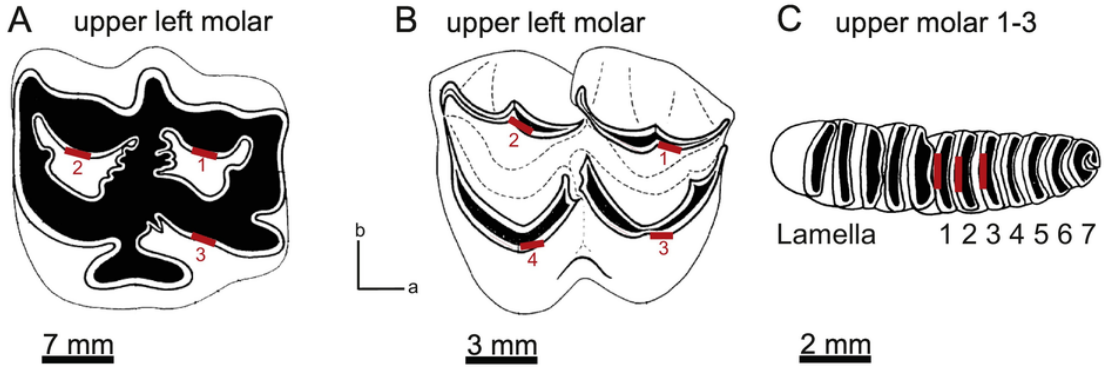

Fig. 1. Schematic representation of the tumbled specimens. A: Upper left molar of *Equus* sp. with the three possible facets (red bars). B: Upper left molar of *Capreolus capreolus* with the four possible facets (red bars). C: Upper molar 1–3 of *Otomys* sp. with the possible lamellae on the third molar (red bars). Occlusal tooth views modified after Thenius (1989). (For interpretation of the references to colour in this figure legend, the reader is referred to the web version of this article.)

UNCORRECTED PROOF

Table 1
Tumbled specimens with tooth side and position (where possible), analysed facet (see Fig. 1), grain size fraction and tumbling interval.

Taxon	Side	Tooth position	Facet	Original vs. mould	Treatment	Tumbling interval [hrs]
Equus sp.	right	M2	3	original	63–125 μm	0.5, 1, 2, 4, 8, 12, 16, 336
Equus sp.	right	M1	1	original	63–125 μm	
Equus sp.	left	M2	1	original	63–125 μm	
Equus sp.	left	P4	1	original	125–250 μm	
Equus sp.	right	P4	1	original	125–250 μm	
Equus sp.	left	M1	3	original	125–250 μm	
Equus sp.	left	P3	1	original	250–500 μm	
Equus sp.	right	P3	3	original	250–500 μm	
Equus sp.	left	P2	1	original	250–500 μm	
Capreolus capreolus	left	M1	2	original	63–125 μm	4, 8, 12, 16, 336
Capreolus capreolus	left	P2	3	original	63–125 μm	
Capreolus capreolus	right	M3	1	mould	63–125 μm	
Capreolus capreolus	left	M2	3	original	125–250 μm	
Capreolus capreolus	left	P3	4	original	125–250 μm	
Capreolus capreolus	right	P4	1	original	125–250 μm	
Capreolus capreolus	left	M3	4	original	250–500 μm	
Capreolus capreolus	left	P4	4	original	250–500 μm	
Capreolus capreolus	right	M1	3	original	250–500 μm	
Otomys sp.	n.n	n.n	L1	original	63–125 μm	4, 8, 12, 16
Otomys sp.	n.n	n.n	L1	original	63–125 μm	
Otomys sp.	n.n	n.n	L2	original	63–125 μm	
Otomys sp.	n.n	n.n	L1	original	125–250 μm	
Otomys sp.	n.n	n.n	L2	original	125–250 μm	
Otomys sp.	n.n	n.n	L2	original	125–250 μm	
Otomys sp.	n.n	n.n	L1	original	250–500 μm	
Otomys sp.	n.n	n.n	L1	original	250–500 μm	
Otomys sp.	n.n	n.n	L1	original	250–500 μm	

potential alteration effects on diet-related ante-mortem textures occurring during the first hours (i.e. first kilometres) of simulated fluvial transport. Additionally, teeth of two species (*C. capreolus* and *Equus* sp.) were also tumbled for 336 h to simulate a long distance (362.9 km) transport scenario. The enamel texture of each tooth was scanned prior to tumbling, to establish baseline parameters and document original ante-mortem dental wear. Approximately the same surface area was scanned again after each time interval of tumbling (Table 1).

2.4. Data acquisition for enamel surface texture analysis

The surface scans of occlusal enamel facets were performed using the high-resolution disc-scanning confocal 3D-surface measuring system μsurf Custom (NanoFocus AG, Oberhausen, Germany) with a blue LED (470 nm) and high-speed progressive-scan digital camera (984 x 984 pixel), following the procedure described in Schulz et al. (2010). A square area of 160 × 160 μm was scanned using the x100 long distance lens (numerical aperture 0.8) with a resolution in x, y = 0.16 μm, and z = 0.06 μm. Measurements with a vertical displacement range $\delta z > 60$ μm were rejected (i.e. measured surface was oriented too obliquely).

We applied 3D (enamel) surface texture analysis (compare Schulz et al., 2010, 2013a, 2013b; Calandra et al., 2012) and scale-sensitive fractal analysis (SSFA) using parameters after Ungar et al. (2003) and Scott et al. (2006) using MountainsMap Premium v.7.4.8676 software for data evaluation. To test for the impact of imprecision in misalignment of repeated sampling, we performed a nine-time repetition of the same scan for one original and one moulded sample. Percentage variance was below 1% for ~50°% (moulded sample) and ~57% (original sample) of the parameters. For the parameters *Spd*, *S10z*, *S5p*, *S5v*, *Shv*, *mea,* and *madf* a percentage variance above 10°% (Table S1) was found.

2.5. Data processing

2.5.1. Dental microwear texture analysis

The measurements were processed using two different templates in MountainsMap Premium v.7.4. 8495 (DigitalSurf, Besançon, France):

1. *Otomys* template. First an extraction sub-surface of 60 × 60 μm was cut out using the extraction operator in MountainsMap, because the enamel bands of this taxon are smaller than the typical measurement field of 160 × 160 μm used for all other teeth. All extracted scans of *Otomys* sp. were treated in the same way without mirroring to account for left/right teeth, since tooth position could not be determined. Most surface texture parameters are, however, expected not to differ between left and right teeth with exception of directional parameters such as *Str*, *Spd*, *Tr1R*, *Tr2R*, *Tr3R*. After tumbling, we expect directional parameters to be altered and hence the inclusion of both left and right teeth with potentially different original surface textures is unproblematic.
2. Large mammal template. This template is designed to analyse scans on original upper right (pre-) molar teeth. Therefore, in order to have the same orientation in all teeth, all scans of original left teeth were mirrored along the y-axis. All moulded surfaces were mirrored along the z-axis, since the measurements first need to be inverted, additionally, all moulded upper right teeth need to be mirrored along the x-axis.

The analysis is based on 3D industrial area surface texture standards (ISO 25178, ISO 12781), with parameters which allow quantification of an area based on surface texture geometry (Schulz et al., 2010; Calandra et al., 2012). Thirty-five 3D-surface roughness parameters (according to ISO 25178): standardised height, functional, spatial, hybrid, and segmentation parameters (Schulz et al., 2013b); and fourteen motif, furrow, isotropy, and ISO 12781 (flatness) parameters integrated in Mountains 7.4 were computed (Table 2). Additionally, we employed the SSFA parameter *Asfc* (complexity) and *epLsar* (anisotropy) (compare Ungar et al., 2007, 2008), as these are commonly applied to differentiate browsing and grazing herbivores (Scott et al., 2005, 2006; Merceron et al., 2007; DeSantis et al., 2013; Ungar et al., 2012).

UNCORRECTED PROOF

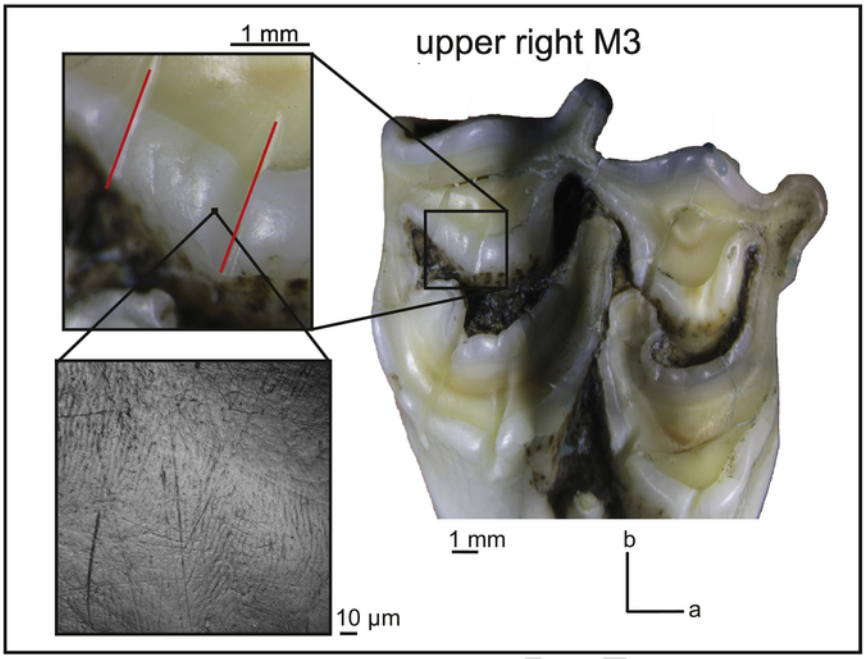

Fig. 2. Exemplary graphical representation of the measurement position on the chewing facet of the upper third molar (M3) of *Capreolus capreolus*; and the cut marks (red lines) used for orientation. The area of the 3D scan is 160 × 160 µm. b = buccal, a = anterior. (For interpretation of the references to colour in this figure legend, the reader is referred to the web version of this article.)

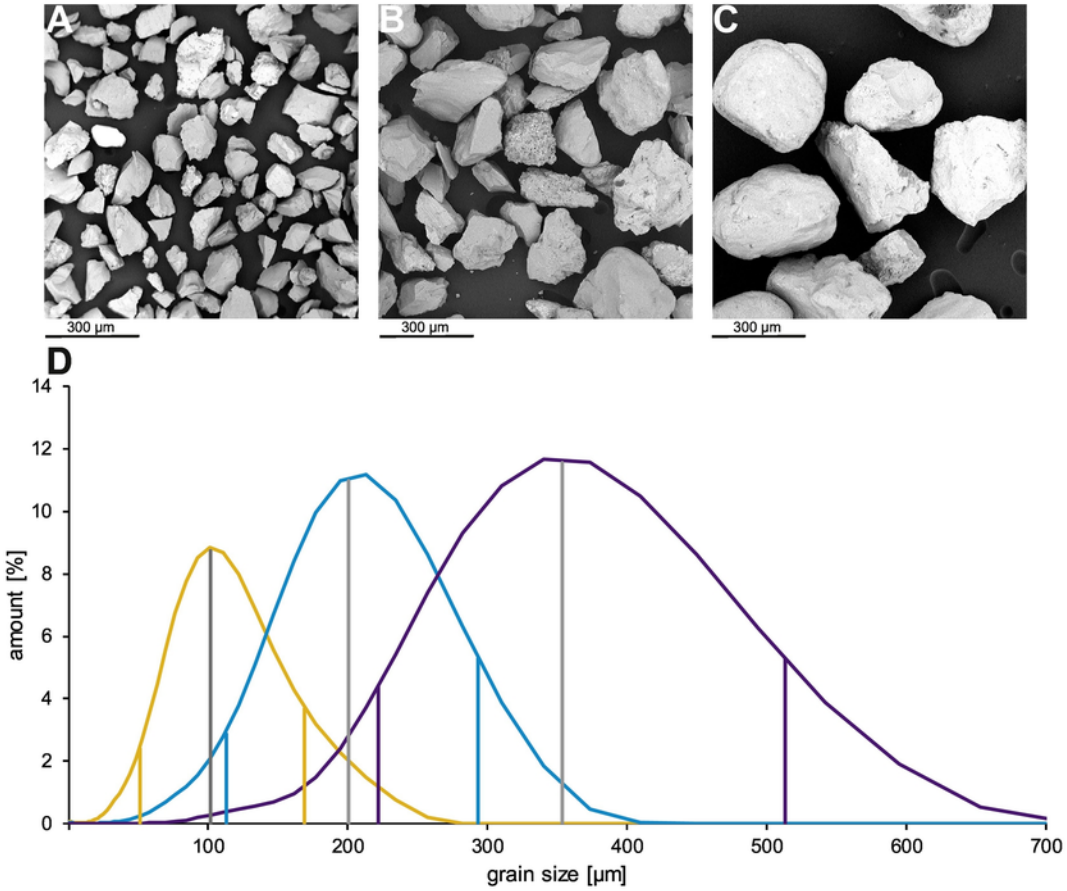

Fig. 3. Graphical representation of the sediment grain size fractions measured by laser granulometry. SEM photos (275× magnification) of A: very fine sand, median 101 µm (range: 51–168 µm); B: fine sand, median 200 µm (range: 112–292 µm); and C: medium sand, median 353 µm (221–513 µm). D: Grain size distribution according to analysis with laser granulometry. Yellow = very fine sand (51–168 µm), blue = fine sand (112–292 µm), violet = medium sand (221–513 µm). (For interpretation of the references to colour in this figure legend, the reader is referred to the web version of this article.)

Table 2
Description of applied surface texture parameters according to ISO 25178, ISO 12781, motif, furrow, texture direction and isotropy.

Category	Parameter	Description (condition)	Standard	Unit
Height	*Sq*	Standard deviation of the height distribution, or RMS surface roughness	ISO 25178	µm
	Ssk	Skewness of the height distribution	ISO 25178	no unit
	Sku	Kurtosis of the height distribution	ISO 25178	no unit
	Sp	Maximum peak height, height between the highest peak and the mean plane	ISO 25178	µm
	Sv	Maximum pit height, depth between the mean plane and the deepest valley	ISO 25178	µm
	Sz	Maximum height, height between the highest peak and the deepest valley	ISO 25178	µm
	Sa	Arithmetic mean height or mean surface roughness	ISO 25178	µm
Function	*Smr*	Areal material ratio	ISO 25178	%
	Smc	Inverse areal material ratio (p = 10%)	ISO 25178	µm
	Sxp	Peak extreme height difference in height between p% and q% (p = 50%, q = 97.5%)	ISO 25178	µm
	Sk	Core height	ISO 25178	µm
	Svk	Reduced dale height, average height of the protruding dales below the core surface	ISO 25178	µm
	Spk	Reduced peak height, average height of the protruding peaks above the core surface	ISO 25178	µm
	Smr1	Peak areal material ratio	ISO 25178	%
	Smr2	Dale areal material ratio	ISO 25178	%
Spatial	*Sal*	Auto-correlation length (s = 0.2)	ISO 25178	µm
	Str	Texture aspect ratio (s = 0.2)	ISO 25178	no unit
	Std	Texture direction	ISO 25178	no unit
Hybrid	*Sdq*	Root mean square gradient	ISO 25178	no unit
	Sdr	Developed interfacial area ratio	ISO 25178	%
Volume	*Vm*	Material volume at a given material ratio (p = 10%)	ISO 25178	µm³/µm²
	Vmc	Material volume of the core at given material ratio (p = 10%, q = 80%)	ISO 25178	µm³/µm²
	Vmp	Material volume of the peaks (p = 10%)	ISO 25178	µm³/µm²
	Vv	Void volume at a given material ratio (p = 10%)	ISO 25178	µm³/µm²
	Vvc	Void volume of the core (p = 10%, q = 80%)	ISO 25178	µm³/µm²
	Vvv	Void volume of the valley at a given material ratio (p = 80%)	ISO 25178	µm³/µm²
Feature	*S10z*	Ten-point height	ISO 25178	µm
	S5p	Five-point peak height	ISO 25178	µm
	S5v	Five-point valley height	ISO 25178	µm
	Sda	Closed dale area	ISO 25178	µm²
	Sdv	Closed dale volume	ISO 25178	µm³
	Sha	Closed hill area	ISO 25178	µm²
	Shv	Closed hill volume	ISO 25178	µm³
	Spc	Arithmetic mean peak curvature	ISO 25178	1/µm
	Spd	Density of peaks	ISO 25178	1/µm²
Motif	*nMotif*	Number of motifs	Motif	no unit
	meh	Mean height	Motif	µm
	mea	Mean area	Motif	µm²
Furrow	*metf*	Mean depth of furrows	Furrow	µm
	medf	Mean density of furrows	Furrow	cm/cm²
	madf	Maximum depth of furrows	Furrow	µm
Direction	*Tr1R*	First direction	Direction	no unit
	Tr2R	Second direction	Direction	no unit
	Tr3R	Third direction	Direction	no unit
Isotropy	*IsT*	Texture isotropy	Isotropy	%
Flatness	*FLTt*	Peak to valley flatness deviation of the surface (Gaussian Filter, 0.025 mm)	ISO 12781	µm
	FLTp	Peak to reference flatness deviation (Gaussian Filter, 0.025 mm)	ISO 12781	µm
	FLTv	Reference to valley flatness deviation (Gaussian Filter, 0.025 mm)	ISO 12781	µm
	FLTq	Root mean square flatness deviation (Gaussian Filter, 0.025 mm)	ISO 12781	µm
SSFA	*Asfc*	Fractal complexity (Area-scale)	SSFA	no unit
	epLsar	Length-scale anisotropy	SSFA	no unit

2.5.2. Statistics

Two datasets which were subjected to different statistical procedures, are described below. The open-source software R v.3.4.1 (R. Development Core Team, 2009) with the packages xlsx, rJava, doBy, R.utils and WRS version 0.12.1 was used for the statistical analyses. For every specimen, only one measured facet was used. The datasets were calculated equally for all three species (n = 9 teeth) as follows:

1. A mean for each tumbled tooth was calculated from four measured scans for t_0 and for each tumbling interval (Table 1) (n = 9 mean values).
2. Dataset 1 (Table S2), separated after sediment grain size fraction. Here, we used the mean values of step 1 and calculated a mean for each sediment type (n = 3 teeth/mean values).
3. Dataset 2 (Table S3), all nine teeth per taxon were pooled (ignoring the grain size fraction with which it was tumbled during the experiment). Here, we used the mean values of step 1 and averaged these nine values for t_0 and per tumbling interval (Table 1)

For Dataset 1 we only present descriptive statics, because a sample size of n = 3 per species and sediment grain size fraction is not sufficient to draw statistically significant conclusions. However, we discuss visible trends in parameter value development between tumbling intervals. Trends are calculated by the quotient of tumbling time zero (t_0) and the maximum tumbling time (t_{max}) (16 h for *Otomys* sp., 336 for *Equus* sp. and *C. capreolus,* Table S4). If the value for the quotient (index) is above a value of one outside the standard error, the parameter value is increasing and the trend is described as positive. If the quotient (index) value is below one outside the standard error, the trend is de-

UNCORRECTED PROOF

scribed as negative. In case the quotient (index) value is within the standard error, there is no trend in the parameter.

For Dataset 2, we employ pair-wise comparisons of surface texture parameter values within species between the different tumbling intervals. Dataset 2 also allows us to test for conservation of significant differences between dietary categories (grazer – browser). Previous studies have shown that surface texture data is non-normally distributed and heteroscedastic (e.g. Schulz et al., 2013a). Therefore, we used the procedure of Wilcox (Wilcox, 2003, 2005), applying the robust heteroscedastic Welch-Yuen omnibus test (Welch, 1938; Yuen, 1974) coupled with a heteroscedastic pair-wise comparison test ("Lincon test", analogous to Dunnett's T3 test (Dunnett, 1980)). Data were trimmed (15%) to compensate for non-normality. Following the established statistical protocol for 3DST data in dietary analyses (Calandra et al., 2012; Schulz et al., 2013a), we further applied the robust heteroscedastic rank-based test according to Cliff (Cliff, 1996; Schulz et al., 2013a). Due to the heterogeneity of the tooth sample (different tooth positions and suitability of facets for texture analysis), we encountered a higher variability in diet-related texture parameters than in previous studies. This was evident in the results from the rank-based statistical test (Cliff's method) which did not confirm the significant differences documented by the first robust heteroscedastic pair-wise comparison ("Lincon's test").

3. Results

Only texture parameters (Table 2) showing distinct trends after the tumbling intervals are further described (Fig. 5) and only parameters with obvious alterations are plotted for the individual species in Figs. 4, 7 and 8.

3.1. Small mammal-Otomys sp.

3.1.1. Dataset 1: very fine sand (51–168 μm)

Most intra-specific alterations are observed in this grain size fraction. Three parameters, which reflect the extreme height differences of the surface texture, are decreasing (*Sq, Sv* and *Svk*, Fig. 4). All parameters (except of *Str*) showing a negative trend (Fig. 5) (decreasing parameters) are describing the overall surface flatness (*FLTt, FLTp, FLTv, FLTq*), volume (*Vm, Vv, Vmp, Vmc, Vvc, Vvv*), roughness (*Sa*), dales and peaks (*Spd, Spc, S5p, S5v, Shv, Sdv, madf, metf*). Complexity (*Asfc*) vs. heterogeneity (*epLsar*) of the surface texture (Fig. 6) is decreasing during the first 4 h of tumbling, during the last 12 h of tumbling, no further alteration was observed.

3.1.2. Dataset 1: fine sand (112–292 μm)

Peaks become less voluminous as indicated by decreasing *Vm* and *Vmp* (Fig. 4), while the volume of valleys and core (*Vv, Vvc, VVv, Vmc,* Fig. 5) remained almost unaltered after the treatment with the fine sand. The majority of altered parameters (describing overall height and roughness; *Sq, Sa*) show a negative trend for parameter values over the 16 h of tumbling (Fig. 5). The parameter related to size of dales (*Sdv*) has an increasing trend. *Asfc* vs. *epLsar* does not change during the course of all tumbling intervals (Fig. 6).

3.1.3. Dataset 1: medium sand (221–513 μm)

Similar to the two smaller grain size fractions, parameters describing the volume (*Vm, Vv, Vmp, Vmc, Vvc*), general height (*meh, Sq*) and the extreme features (peaks and dales; *Spc, S5p, S5v, Shv*) tend to de-

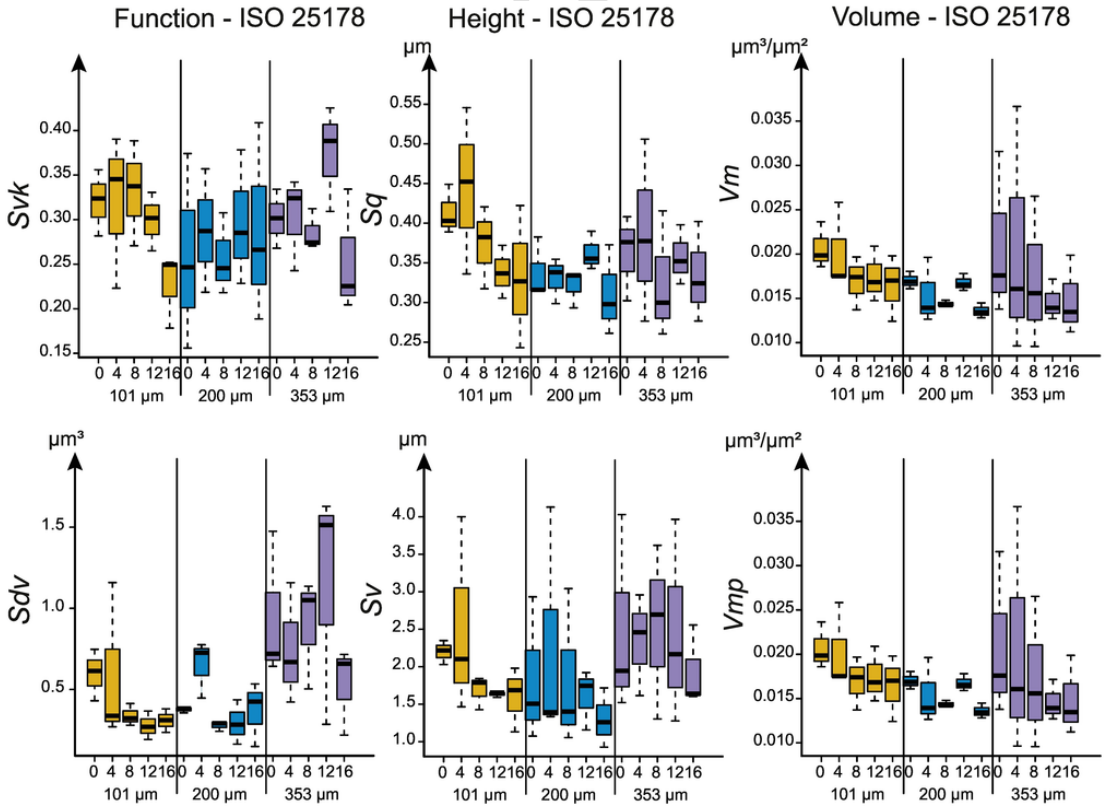

Fig. 4. Examples of parameters with strong alteration after tumbling (Dataset 1) of *Otomys* sp.. Yellow = Very fine sand (51–168 μm), blue = Fine sand (112–292 μm), violet = Medium sand (221–513 μm). *Svk* = Reduced dale height, *Sq* = Standard deviation of the height distribution, *Vm* = Material volume at a given material ratio (p = 10%), *Sdv* = Closed dale volume, *Sv* = Maximum pit height, depth between the mean plane and the deepest valley, *Vmp* = Material volume of peaks (p = 10). (For interpretation of the references to colour in this figure legend, the reader is referred to the web version of this article.)

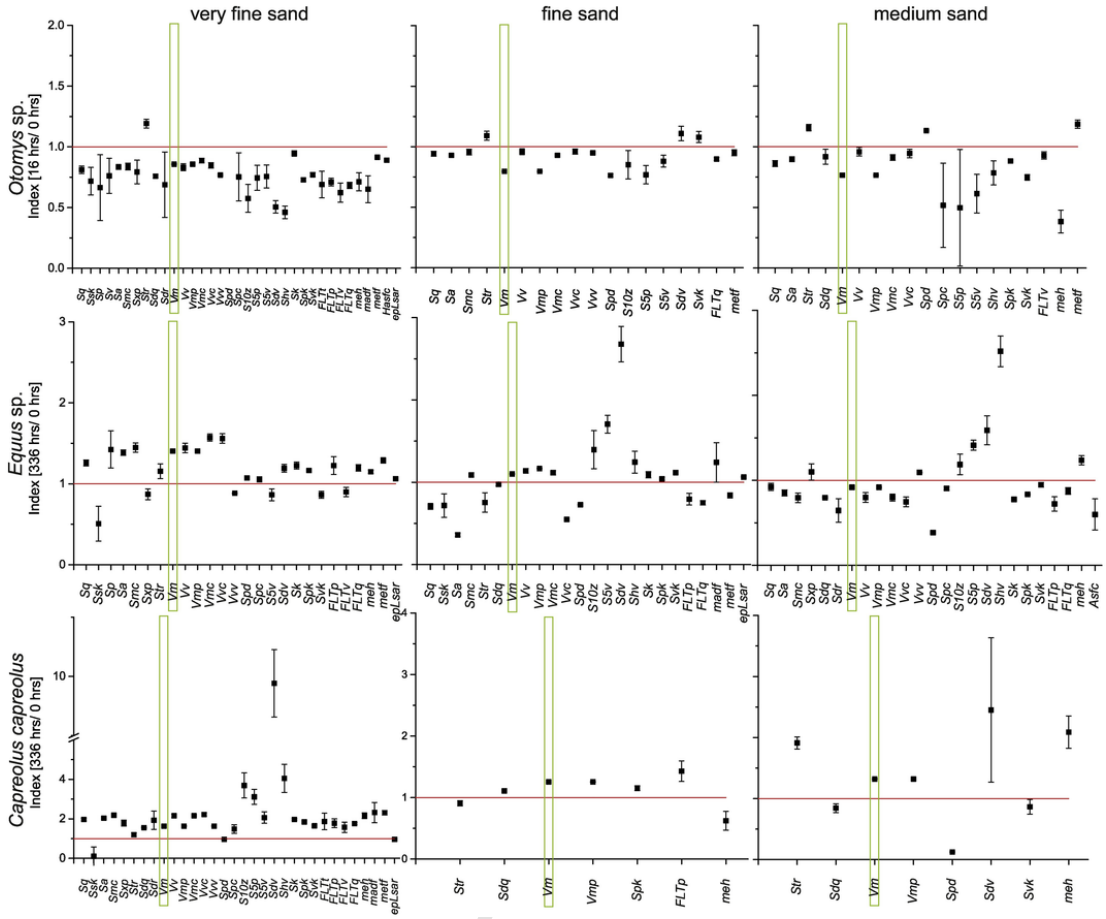

Fig. 5. Trends for Dataset 1 *of Otomys* sp., *Equus* sp. and *C. capreolus*. Index values of t_0 calculated with standard error. Red line = Index value of one. The roughness parameter *Vm* (material volume) shows an index value different from 1 in all treatments (within the standard error), and therefore highlighted to illustrate the intraspecific trends. For *Otomys* sp., *Vm* shows a negative trend (index value below 1) in all three grain size fractions, *Vm* decreases from t_0 to t_{max}. In *Equus* sp. *Vm* increase from t_0 to t_{max} for the two smaller grain size fractions, the index values are above 1. However, for the medium sand, the trend is negative (index value below 1), *Vm* value of t_{max} is lower than t_0. For *C. capreolus Vm* shows an increasing trend in all grain size fractions (index values above 1), *Vm* values are higher in t_{max} than t_0. (For interpretation of the references to colour in this figure legend, the reader is referred to the web version of this article.)

crease (Fig. 5). *Asfc* vs. *epLsar* is not altered after the tumbling treatment with the medium sand (Fig. 6).

3.2. Large mammals-Equus sp.

The *Equus* sp. (pre-)molars are the only large mammal teeth which show pronounced alterations after the tumbling process.

3.2.1. Dataset 1: very fine sand (51–168 μm)

In this size fraction almost no alteration on the inner wear facets is observed, even though the tumbled teeth macroscopically display pronounced rounding of cusps and other elevations of the occlusal surface and visible alteration on the facets after 336 h of tumbling (Fig. 9). After a tumbling time of 336 h, reflecting a transport distance of over 360 km, parameters describing the surface volume (*Vm, Vv, Vmp, Vmc, Vvc*) and general surface roughness (*Sa*) show positive trends (Fig. 5). Increasing values are found primarily in the peak and dale parameters (*Sp, Spd, Spc, S5v, Spk, metf*) and additionally in parameters describing the general height (*meh*) (Fig. 5). Negative trends are found in *Ssk, Sxp, Vvv, S5v, Svk* and *FLTv*. Regarding *Asfc* vs. *epLsar*, both parameters increase after ~540 m of transport (30 min of tumbling), however, for longer tumbling intervals no further alteration is visible (Fig. 6).

3.2.2. Dataset 1: fine sand (112–292 μm)

Equus sp. teeth show strong signs of alteration in surface texture (Fig. 7). In contrast to the smaller grain size fraction, the whole chewing area shows no obvious macroscopic alteration at the corners. *medf* decreases over the whole tumbling treatment of 336 h, while the ISO void volume parameter (*Vv*) increases (until 16 h of tumbling) (Fig.7). A positive trend is observed in parameters describing the overall volume (*Vm, Vmp, Vmc, Vvc*) and a strong negative in the general surface roughness (*Sa*) and height (*Sq*) (Fig. 5). Parameters describing peaks and dales (*Spd, S10z, S5v, Sdv, Shv, Spk, Svk, madf, metf*) of the surface are ambiguous (Fig. 5).

3.2.3. Dataset 1: medium sand (221–513 μm)

Parameters describing the amount of the dales (*medf,* Fig. 7) and the complexity (*Asfc,* Fig. 6) decrease over the whole tumbling time (336 h). Only seven parameters show a positive trend (*Sxp, Vvv, S10z, S5p, Sdv, Shv* and *meh*), while parameters describing the volume (*Vm, Vv, Vmp, Vmc, Vvc*) and the peaks (*Spd, Spc,)* as well as the general roughness (*Sa*) decrease in their parameter values over ~362 km of transport (336 h of tumbling) (Fig. 5).

UNCORRECTED

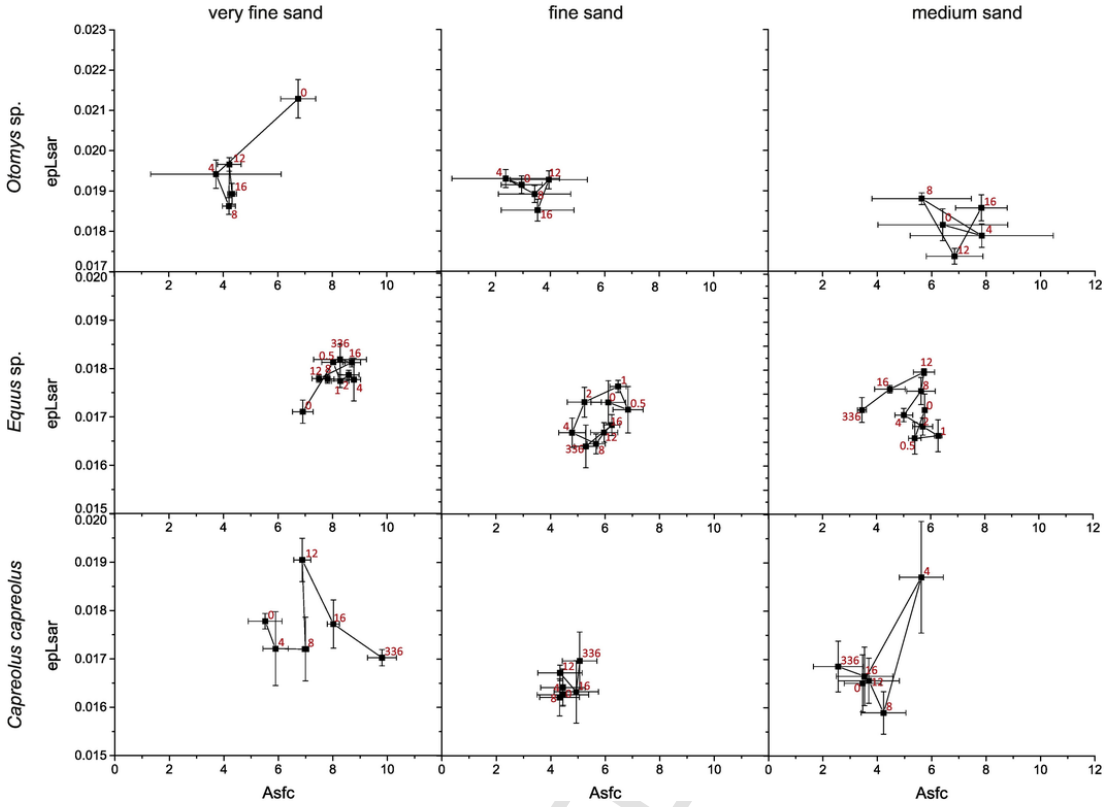

Fig. 6. Complexity vs. heterogeneity for Dataset 1 of *Otomys* sp., *Equus* sp. and *C. capreolus* at all tumbling intervals (red numbers represent the hours of tumbling). (For interpretation of the references to colour in this figure legend, the reader is referred to the web version of this article.)

3.3. Large mammals-Capreolus capreolus

The roe deer teeth do show alteration in parameter values and new wear features are visible after tumbling procedure (described below).

3.3.1. Dataset 1: very fine sand (51–168 μm)

The strongest alteration effect on enamel facets can be observed for this grain size fraction (Figs. 5 and 8). *Ssk, Spd* and *epLsar* are the only parameters showing a negative trend over 336 h of tumbling, while the parameters describing the volume (*Vm, Vmp, Vmc, Vvc, Vvv* (Fig. 5), *Vv* (Fig. 8)), the general surface texture (*Sq, Sa, Sxp, Str* (Fig. 5), *Smc* (Fig. 8)), the dales and peaks (*S10z, S5p, S5v, Sdv, Shv, madf* (Fig. 5), *Spc, metf* (Fig. 8)) increase. *Asfc* vs. *epLsar* of specimens tumbled with this grain size fraction show a broad range of values between the different tumbling intervals (Fig. 6).

3.3.2. Dataset 1: fine sand (112–292 μm)

The least alteration during the tumbling experiment was found for the fine sand fraction (112–292 μm). The teeth of *Capreolus capreolus* show a pronounced negative trend in two surface texture parameters, *Str* and *meh* (Fig. 5). A positive trend is found in five parameters describing the peaks (*Spk, FLTp*) and the volume (*Vm, Vmp*) (Fig. 5).

3.3.3. Dataset 1: medium sand (221–513 μm)

Teeth tumbled with this grain size fraction of medium sand show an obvious surface abrasion already visible with the naked eye (Fig. 9). However, only eight surface texture parameters show pronounced trends. *Sdq, Spd* and *Svk* decrease strongly, while parameters *Str, Vm, Vmp, Sdv* and *meh* increase (Fig. 5), comparable to the trends observed in the roe deer specimens tumbled with the fine sand. After four hours of tumbling, *Asfc* vs. *epLsar* increases strongly, but then reverts back to the level of time zero during all remain tumbling intervals until 336 h (Fig. 6).

3.4. Large mammals Dataset 2-grazer versus browser

3.4.1. Conservation of inferred diet categories at the same tumbling interval

The parameter differences between zebra and roe deer remain stable for the majority of well-differentiating parameters. Overall, in both species alteration is only visible as non-significant trends, which are however more pronounced in *C. capreolus* teeth (Dataset 2) compared to *Equus* sp. (Dataset 2). All ISO 25178 volume parameters are altered towards increasing values for both species (zebra and roe deer), leading to consistently higher parameter values *Vmc, Vvv, Vv* and *Vvc* (example parameter *Vv* Fig. 10) in the grazer (*Equus* sp.). Additionally, the ISO 12781 flatness parameters (*FLTp, FLTq* (example parameter *FLTq* Fig. 10)) and the well separated ISO 25178 parameters *Smc, Sxp and Sa* (Fig. 10) of the grazer (*Equus* sp.) are consistently higher than those of the browser (*C. capreolus*) and lower in *medf* (Fig. 10).

3.4.2. Diet categories between different tumbling intervals

Besides finding differences between grazer (*Equus* sp.) and browser (*C. capreolus*) at the same tumbling interval, these two diet categories are also still distinguishable when original tooth surface textures are compared to those of tumbled samples (Fig. 10).

After t_{16}, surface textures of tumbled *C. capreolus* still show smaller flatness parameters (*FLTp, FLTq, FLTt* (example parameter *FLTq* Fig. 10)) and ISO 25178 roughness parameters *Sa, Smc,* the volume parameters (*Vmc, Vv* and *Vvc* (example parameter *Vv* Fig. 10)) than the untreated *Equus* sp. samples (Fig. 10). After t_{336} of tumbling, only four separating parameters still show pronounced differences between the two diet categories. The flatness parameter *FLTq,* and the parameters *Sa, Sxp* and *Vmc* (Fig. 10) still separate clearly.

UNCORRECTED

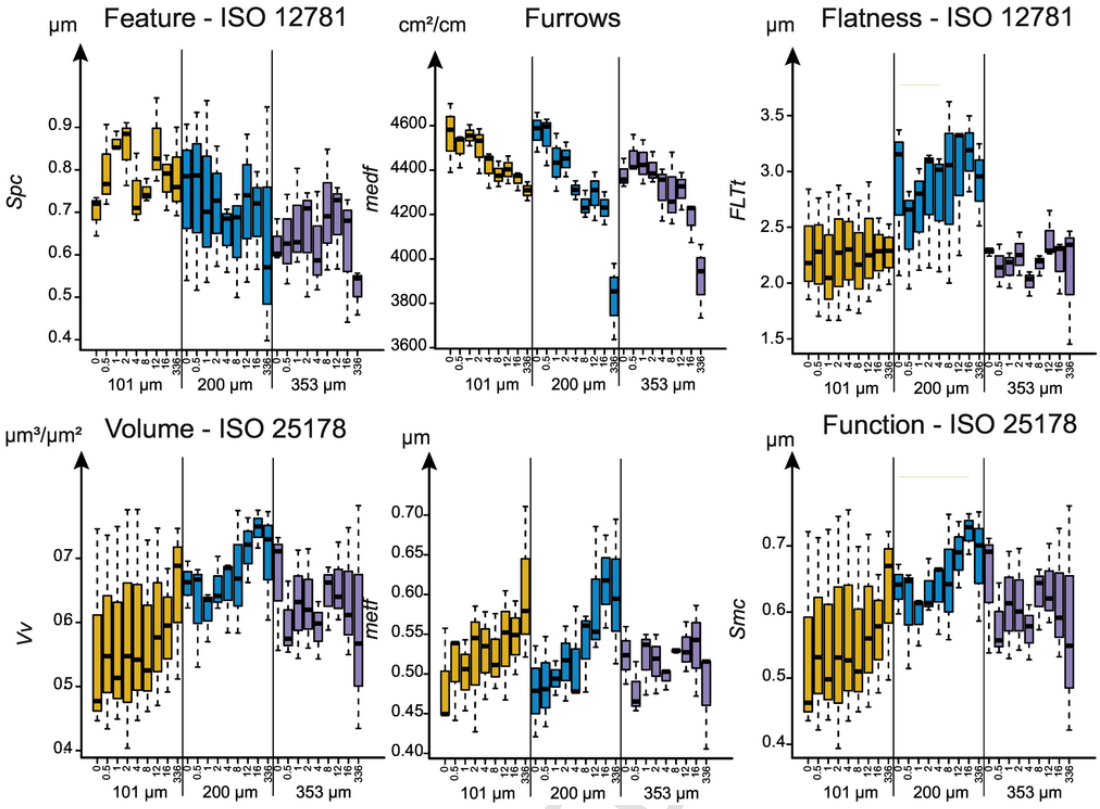

Fig. 7. Examples of parameters with strong alteration after tumbling (Dataset 1) of *Equus* sp.. Yellow = very fine sand (51–168 µm), blue = fine sand (112–292 µm), violet = medium sand (221–513 µm). *Spc* = Arithmetic mean peak curvature, *medf* = Mean density of furrows, *FLTt* = Peak to valley flatness deviation of the surface, *Vv* = Void volume at a given material ratio (p = 10%), *metf* = Mean depth of furrows, *Smc* = Inverse areal material ratio (p = 10). (For interpretation of the references to colour in this figure legend, the reader is referred to the web version of this article.)

Contrary, at t_{16} a higher number of parameters distinguishes the teeth of the grazer (*Equus* sp.) from the teeth of the untreated (pre-tumbled) browser (*C. capreolus*). The values of the surface texture parameters of *Equus* sp. are lower in *medf* than for the browser, even after 336 h of tumbling (Fig. 10). Flatness (*FLTp, FLTq, FLTt* (exemplary parameter *FLTq* Fig. 10)), volume (*Vmc, Vv, Vvc* (exemplary parameter *Vv* Fig. 10)), *Sa* and the function parameters *Sxp* and *Smc* are almost unaltered after the whole tumbling treatment and higher in *Equus* sp. (Fig. 10, *FLTp, FLTt, Vmc* and *Vvc* in Table S2).

4. Discussion

Generally, we observe two different patterns in parameter values when comparing the original, unaltered surface textures with those after the subsequent tumbling intervals. "Stable" parameters are either not significantly altered by the tumbling process or follow a distinct trend with increasing tumbling time (Fig. 11). "Unstable" parameters show pronounced different values after tumbling and/or follow no distinct trend, alternating between increasing and decreasing parameter values over the tumbling intervals (Fig. 12). We find the highest number of stable parameters in the tumbling regimes using the two smaller grain size fractions (51–168 µm, 112–292 µm). Altogether, those parameters that appear to be unstable, in all tumbling regimes, regardless of grain size fraction, describe the extreme height and depth characteristics of the enamel surface (peaks and dales). The peaks are most exposed to the sediment, and therefore vulnerable for alteration through abrasion. However, it needs to be taken into account, that some of these unstable parameters are also prone to measurement inconsistencies in repeated measurement approach (see Table S1). It is clear that observed post-tumbling alteration in parameter values for the parameters *Spd*, *S10z*, *S5p*, *S5v*, *Shv*, *mea*, and *madf* result from experimental abrasion or are due to the repeated measurement error. However, in all other 44 parameters, the error due to repeated measurements is lower than 5%. Changes in these parameters are therefore considered to be the result of the experimental abrasion.

4.1. Differences in sand grain size fractions

4.1.1. Small mammal-Otomys sp.

Otomys sp. are specialised herbivores which live in Africa feed primarily on grasses, reeds and sedges (as well as some fruits, roots and bark) (Skinner and Chimimba, 2005; Happold, 2013). Their 3DST is similar to that of rats from an abrasive, dusty environment in SW Madagascar (Winkler et al., 2016). Tumbling in three different grain size fractions results in relatively small alteration effects on the enamel surface. The most general changes caused by the tumbling procedure, that applies for all grain size fractions, is observed in the volume and height of the peaks and size of the dales (Fig. 13), as indicated by decreasing *Vm* and *Vmp*, *Sp* and *Sv, Sda* and *Sha*. The slightly smaller values for volume parameters, (e.g. the volume of the core (*Vmc*) and the volume of the peaks (*Vmp*)), is likely the result of sediment abrasion (most pronounced in the fine sand) which removed the peaks during the tumbling experiment. In addition, in the two smallest grain size fractions (51–168 and 292 µm), new scratches formed (indicated by increasing *medf)*. However, these scratches are never as deep or as broad (decreasing *Sda*) as those related to ante-mortem wear (Fig. 13). This can possibly be explained by the small size of *Otomys* enamel lamella, which are $<$80 µm wide. The likelihood of sediment particles leaving scratches on the lamella increases with smaller particle size and decreases with larger particle size. In our case, the 51–168 and 112

UNCORRECTED

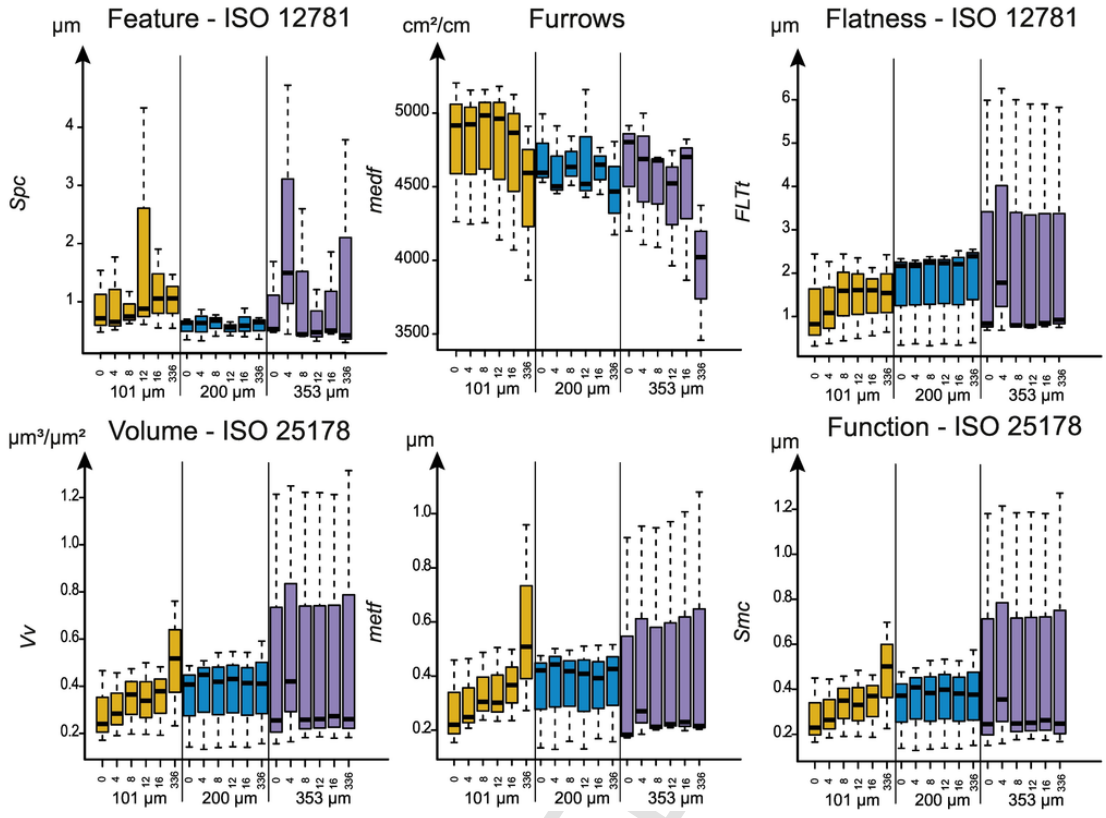

Fig. 8. Examples of parameters (Dataset 1) of *Capreolus capreolus*. Yellow = very fine sand (51–168 µm), blue = fine sand (112–292 µm), violet = medium sand (221–513 µm). *Spc* = Arithmetic mean peak curvature, *medf* = Mean density of furrows, *FLTt* = Peak to valley flatness deviation of the surface, *Vv* = Void volume at a given material ratio (p = 10%), *metf* = Mean depth of furrows, *Smc* = Inverse areal material ratio (p = 10). (For interpretation of the references to colour in this figure legend, the reader is referred to the web version of this article.)

–292 µm grain size fractions were more effective in producing this abrasive signal on these small specimens.

4.1.2. Large mammals-Equus sp.

In contrast to the *Otomys* sp. teeth, the zebra teeth show different patterns of alteration in all the three different grain size fractions. Larger particles have greater potential to leave scratches on the broader enamel bands of the zebra (Fig. 13). Thus, in addition to the abrasion of peaks, a formation of new scratches in all grain size fractions was caused by the tumbling. There is an increase of the volume of the surface texture in the two smaller grain size fractions, and a decrease of the general surface roughness in the two larger grain size fractions. Apart from a slight polishing effect that occurs in all grain size fractions (Fig. 13), and a slightly changing roughness, volume and width of the furrows, teeth of *Equus* sp. show few signs of surface texture alteration, after a long distance (> 360 km) fluvial transport (as simulated in the 336 h experiment), even though the teeth exhibit macroscopic signs of strong abrasion. The least pronounced alteration was observed during tumbling with the very fine sand (51–168 µm), which caused deepening of furrows (increasing *metf*) after 362 km of transport, the surface tends to become more rough and voluminous. Tumbling with the medium sand (221–513 µm) resulted in faster and more intense abrasion of the enamel surface, leading to a less rough and voluminous surface texture (Fig. 13).

4.1.3. Large mammals-Capreolus capreolus

The teeth of the *Capreolus capreolus* do not show pronounced changes of the surface textures in any of the grain size fractions used for the tumbling procedure. Compared to the *Equus* sp. samples, the very fine sand mainly produces deeper scratches on the occlusal surface, while the fine sand only abrades the surface (decreasing *meh*) (Fig. 13). In contrast to the *Equus* sp. teeth, the strongest alteration trends are observed for the very fine sand (51–168 µm). The pre-existing furrows become deeper (increasing *metf* and *madf*), resulting in a relatively increased peak- and mean height and a slightly rougher surface. There is almost no macroscopically visible alteration in the fine sand (112–292 µm), however, surface texture parameters are more level, less textured tooth surface due to peak abrasion.

4.2. Inter-specific differences in mechanical alteration

4.2.1. Preservation of different sized teeth

Understanding alteration and stability of surface features is crucial to infer how good the experimental setup is as a model for natural transport in a fluviatile system. Tumbling intended to mimic fluviatile transport and being performed in barrels may potentially introduce systematic errors. This is because the likelihood for a sediment particle (including a tooth) to touch the inner wall of the barrel will depend on the geometry of both, the barrel and the particle (i.e. tooth). A fluviatile system does not have these restrictions. Periodic contact with the barrel wall may introduce directionally non-random signals to scars, in particular, when the sediment filling is not turbulently mixed, but rather slides along the wall, just separated by a fluid layer. We propose this effect to be reduced with larger sediment infill amounts, when the diameter of the tumbling barrel is small as compared to the size of the tooth. The reverse should hold true, if the specimen is small in relation to the diameter of the barrel. Nevertheless, the texture signals of small mammal teeth appear particularly less sensitive to post-mortem abrasive alteration and should thus be robust in maintaining their ante-mortem signatures, although they do have the possibility to move more

UNCORRECTED

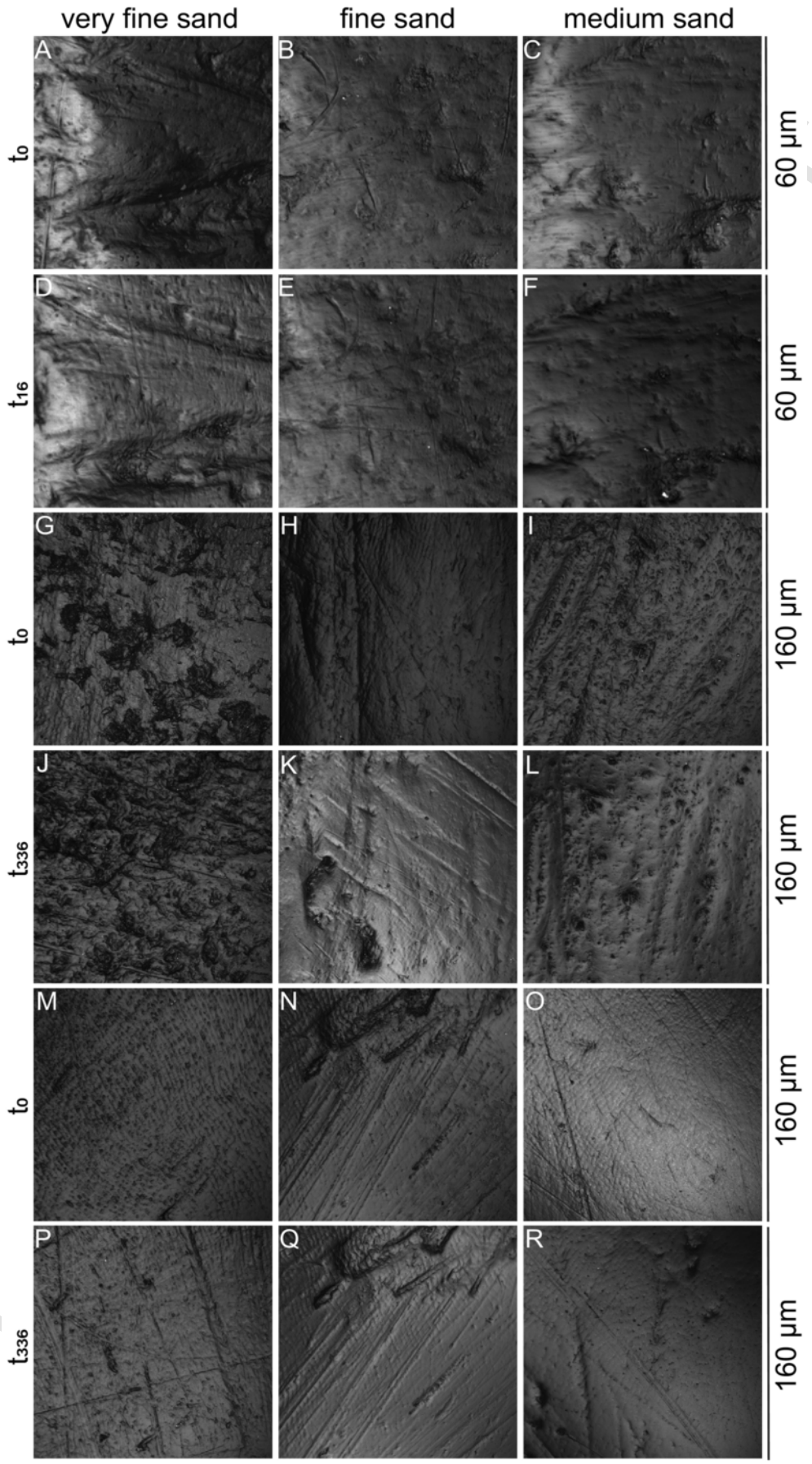
very fine sand
fine sand
medium sand
A
B
C
D
E
F
G
H
I
J
K
L
M
N
O
P
Q
R
t0
t16
t0
t336
t0
t336
60 µm
60 µm
160 µm
160 µm
160 µm
160 µm

◀ **Fig. 9.** Photosimulations 3DTM surface models of single facets of Otomys sp. (A-F), zebra (*Equus* sp.) (G-L) and roe deer (*Capreolus capreolus)*(M-R) teeth. A/D: individual K, lammela 2; B/E: individual J, lamella 2; C/F: indivual L, lamella 1; G/J: upper left M2, facet 1; H/K: upper left M1, facet 3; I/L: upper left P2, facet 1; M/P: upper left M1, facet 2, N/Q: upper left M2, facet 3; O/R: upper right M1, facet 3.

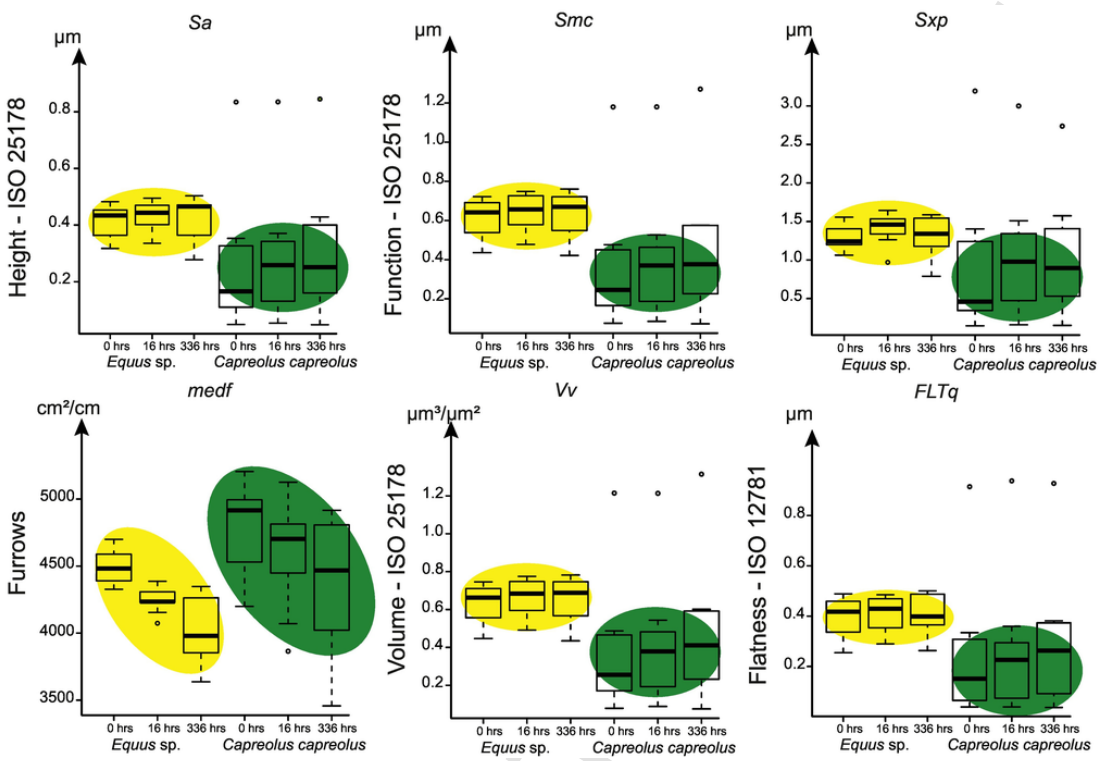

Fig. 10. Well separating 3D surface texture parameters with well distinguished grazer (zebra, yellow) and browser (roe deer, green) specimens. Small open circles represent outliers. *Sa* = Mean surface roughness; *Smc* = Inverse areal material ratio ($p = 10\%$); *Sxp* = Peak extreme height difference in height between $p = 50\%$ and $q = 97.5\%$; *medf* = Mean density of furrows; *Vv* = Void volume at a given material ratio ($p = 10\%$); *FLTq* = Root mean square flatness deviation. (For interpretation of the references to colour in this figure legend, the reader is referred to the web version of this article.)

freely in the barrel, according to the small size of the teeth. This makes them potentially well-suited samples for environmental reconstruction even if the exact post-mortem abrasive impact is unknown.

The zebra teeth tumbled during this experiment show the strongest alteration effects. Considering the geometry of both the barrel and a zebra molar, these large cheek teeth likely overturn along their longitudinal axis, instead of being transported in a randomly oriented fashion in the sediment flow. Our experimental data is thus less well suited to infer fluviatile abrasive effects on such large mammal dental specimens. However, although the roe deer teeth treated during this experiment could potentially move more freely in the barrel than the larger zebra teeth, none of the texture parameters were strongly altered during any of the tumbling treatments. Therefore, medium-sized mammal teeth from fluvial transported fossil assemblages embedded in fine to medium grained siliciclastic sediments, may still preserve their original ante-mortem occlusal surface texture.

4.2.2. Alteration versus preservation of dietary signatures in large mammals

Dietary reconstruction through 3DST is usually applied on homologous tooth positions and enamel wear facets. Due to the composition of the tooth sample set for this partially destructive experiment, the teeth were not ideally suited for dietary analysis, as we compared several wear facets among different tooth positions. Nevertheless, prior to tumbling as well as after the two longest tumbling intervals, grazer and browser could still be distinguished by parameter values (Fig. 10). This supports the applicability of 3DST for dietary reconstruction in fossil species, even on isolated teeth.

Before the tumbling treatment 12 surface texture parameters resulted in excellent separation between grazers and browsers, and nine of these are texture parameters previously demonstrated by Schulz et al. (2013a) to differentiate best between the two feeding traits: *FLTp, FLTq, FLTt, Sa, Smc, Sxp, Vmc, Vv* and *Vvc*. Over a short tumbling period of 16 h, the textural differences between grazers and browsers, especially in these well discriminating parameters, are very stable. In contrast, over the very long tumbling interval of 336 h, four parameters (*FTLp, FLTt, Vv* and *Vvc*) lost their strength in discriminating those two feeding traits. Six surface texture parameters are very stable, mainly corresponding to the volume of the core, the general roughness and the flatness of the surface. Contrary, parameters corresponding to the peaks, dales and the mean height are unstable. In conclusion, isolated teeth from fossil assemblages deposited in siliciclastic sediment by fluviatile transport, with parameters simulated by our experiments, would still preserve diet-related ante-mortem occlusal textures that allow distinction between grazers and browsers. *Vvc, Sa, Smc, Sxp* and *FLTq* would be the best suited parameters in this case. However, those texture parameters characterising extreme topographic features such as peaks and dales, seem to be preferentially biased by abrasive post-mortem alteration and thus are not reliable predictors for ingesta reconstruction under these circumstances. In contrast, if only one species within a comparative pair of two was subject to post-mortem alteration, while the other was not, flatness and volume parameters well as the surface roughness still permit distinction between grazing and browsing. Even if teeth from the same depositional setting are not taphonomically altered in the same way, grazers and browsers should

UNCORRECTED

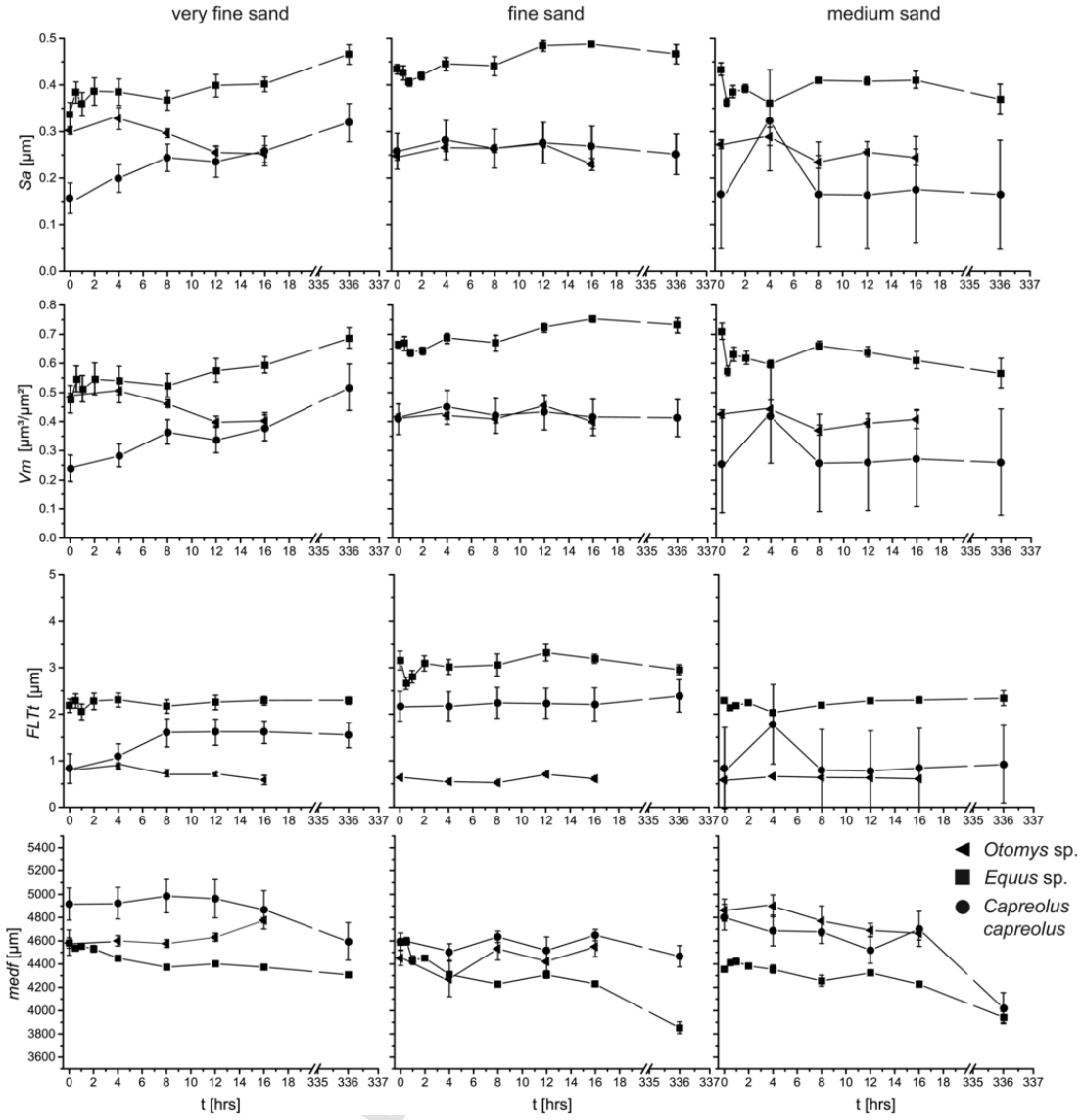

Fig. 11. Examples of stable parameters over the tumbling experiment for Dataset 1 of *Otomys* sp., *Equus* sp. and *Capreolus capreolus*. *Sa* = Mean surface roughness; *Vm* = Material volume; *FLTt* = Peak to valley flatness deviation of the surface; *medf* = Mean density of the furrows.

still be distinguishable in their mostly unbiased texture parameters corresponding to the form and volume of the occlusal surface.

In general, it can be concluded, that discrimination of the two broad dietary categories browser and grazer can still be performed based on surface texture parameters even after a long tumbling period in siliciclastic very fine to medium sand of 336 h (simulating > 360 km of transport distance in a fluviatile environment). This also applies if those teeth that are tumbled in different grain size fractions of sand. Therefore, it is not necessary to categorically exclude fluvial transported dental specimens from dietary reconstruction based on surface texture analysis and likely also other ingesta related dental wear proxies.

5. Conclusion

Tumbling experiments of isolated cheek teeth from large and small mammalian herbivores in siliciclastic sediment demonstrate a high degree of resistance of surface textures against physical post-mortem abrasive alteration during simulated fluvial transport in grain size fractions representing a sandy natural river sediment. The surface texture signatures as measured do not generally respond to post-mortem abrasive alteration as imposed by the tumbling procedure. Macroscopically these modified surfaces appear slightly polished, but we also found newly formed large scratches in different grain size fractions; however, these alteration features do not change the overall surface texture signature significantly. We conclude that there is a difference in the degree of post-mortem abrasive impact related both to sediment particle size and to the morphology and size of an individual dental specimen. Small teeth are less affected compared to larger sized teeth. This effect should relate to the size relation between teeth and sediment grains, where small teeth obviously incur fewer new scratches, if individual grains are at the same size fraction as occlusal enamel structures under study, as indicated by our *Otomys* sample. The larger occlusal facets of the roe deer were most visibly altered in the very fine sand fraction of 51–168 µm, while the zebra samples suffered post-mortem alteration mainly by the coarser grain size fraction of medium sand 221–513 µm grain size fraction. Signs of physical alteration were mainly detected in peak and furrow parameters. No single surface texture parameter could be identified, which can be used as an unambiguous indicator for taphonomic alteration of ante-mortem enamel wear texture. Parame-

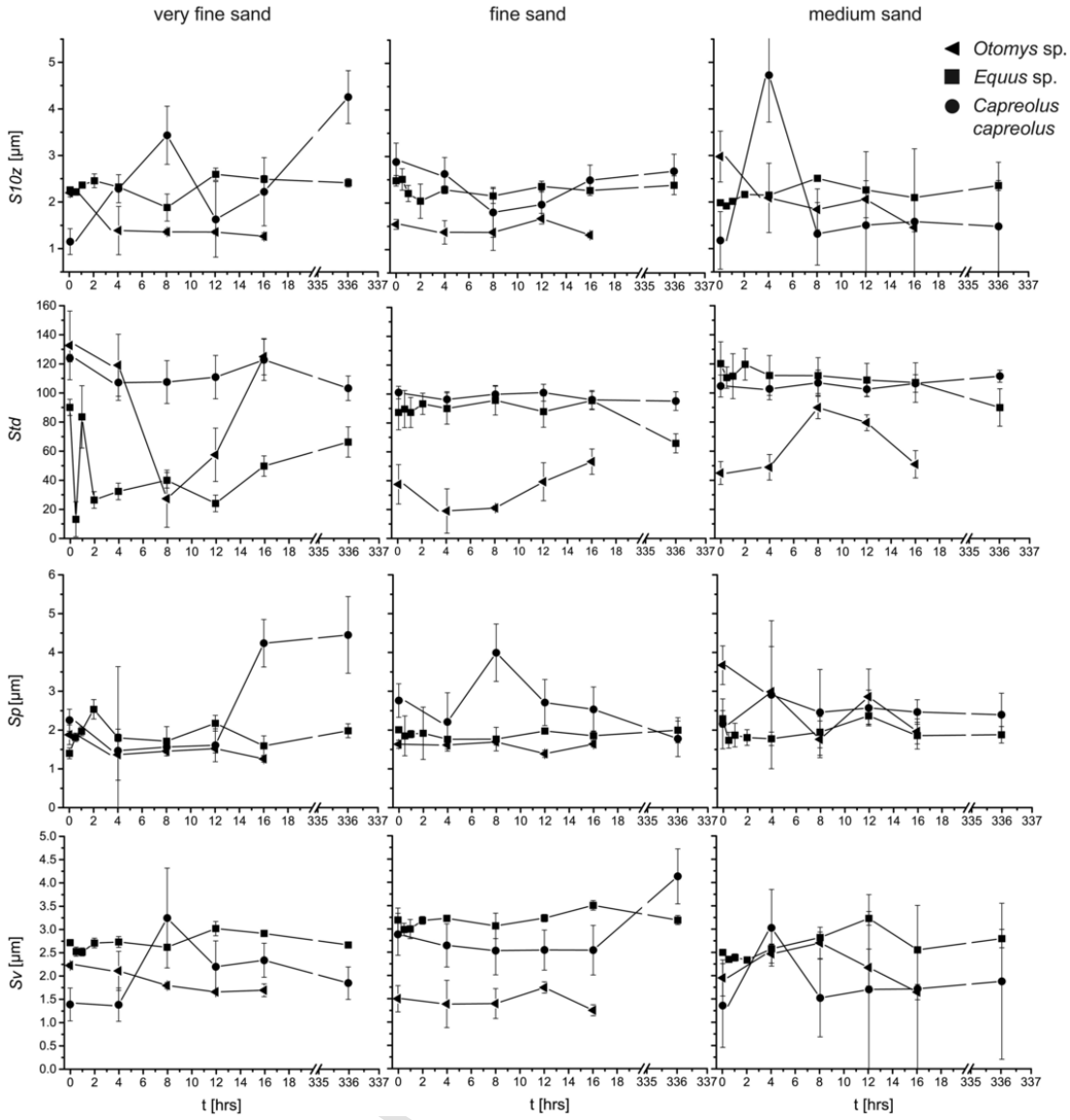

Fig. 12. Examples of unstable parameters over the tumbling experiment for Dataset 1 of *Otomys* sp., *Equus* sp. and *Capreolus capreolus*. *S10z* = Ten-point peak height; *Std* = Texture direction; *Sp* = Maximum peak height; *Sv* = Maximum pit height.

ters describing the volume, flatness and roughness of the wear surface only showed slight shifts. These parameters enable us to discriminate between the two feeding categories, even when isolated teeth of grazers and browsers transported in the same sediment. Therefore, tooth samples need not to be discarded from microtexture analyses even if they are slightly abraded or if the reference tooth position and facet are not preserved, they can still be used for dietary reconstruction, at least to resolve the browser-grazer dichotomy.

Supplementary data to this article can be found online at https://doi.org/10.1016/j.palaeo.2019.01.008.

Uncited reference

Wasserstraßen-und Schifffahrstverwaltung des Bundes, n.d

Acknowledgments

'This project has received funding from the European Research Council (ERC) under the European Union's Horizon 2020 research and innovation programme (grant agreement No 681450) and the Max-Planck Graduate Center. We thank the Center of Natural History (CeNak) and Dr. Irina Ruf (Senckenberg Museum, Frankfurt) for the dental material. We thank Ralf Meffert and Dr. Tobias Häger (Johannes Gutenberg-University Mainz) for the X-ray diffraction-analysis and Prof. Dr. Frank Lehmkuhl (RWTH Aachen University) for the particle size analysis. We would also like to express our gratitude to Dr. Jennifer Leichliter (Johannes Gutenberg-University) for proofreading the manuscript. We further acknowledge the two anonymous reviewers for their helpful comments that greatly helped to improve the manuscript.

UNCORRECTED

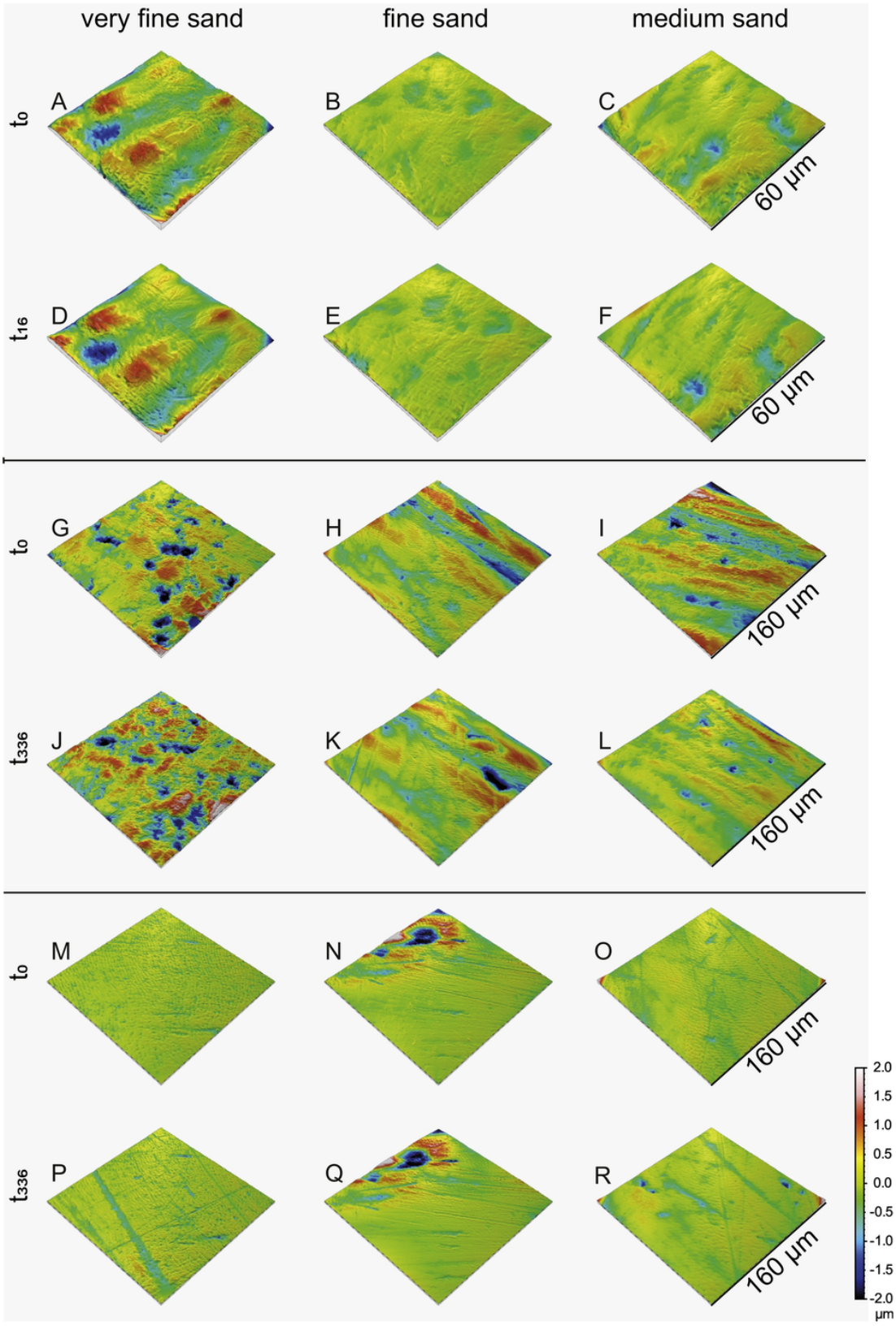

Fig. 13. 3D simulations of surface models of single facets of *Otomys* sp. (A-F), zebra (*Equus* sp.) (G-L) and roe deer (*Capreolus capreolus)* (M-R) teeth. A/D: individual K, lammela 2; B/E: individual J, lamella 2; C/F: indivual L, lamella 1; G/J: upper left M2, facet 1; H/K: upper left M1, facet 3; I/L: upper left P2, facet 1; M/P: upper left M1, facet 2, N/Q: upper left M2, facet 3; O/R: upper right M1, facet 3.

References

Baker, G., Jones, L.H.P., Wardrop, I.D., 1959. Cause of wear in sheep's teeth. Nature 184, 1583–1584.

Calandra, I., Merceron, G., 2016. Dental microwear texture analysis in mammalian ecology. Mammal Rev. 46, 215–228.

Calandra, I., Schulz, E., Pinnow, M., Krohn, S., Kaiser, T.M., 2012. Teasing apart the contributions of hard dietary items on 3D dental microtextures in primates. J. Hum. Evol. 63, 85–98.

Cliff, N., 1996. Ordinal Methods for Behavioral Data Analysis. Erlbaum, Mahwah, New Jersey.

Dahlberg, A.A., Kinzey, W., 1962. Étude microscopique de l'abrasion et de l'attrition sur la surface des dents. Bull. Group Int. Rech. Sci. Stomatol. Odontol. 5, 242–251.

Damuth, J., Janis, C.M., 2011. On the relationship between hypsodonty and feeding ecology in ungulate mammals, and its utility in palaeoecology. Biol. Rev. 86, 733–758.

Dauphin, Y., Andrews, P., Denys, C., Fernánder-Jalvo, Y., Williams, T., 2003. Structural and chemical bone modifications in a modern owl pellet assemblage from Olduvai Gorge (Tanzania). J. Taphonom. 1, 209–232.

Dauphin, Y., Castillo-Michel, H., Denys, C., El Hajraoui, M.A., Nespoulet, R., Stoetzel, E., 2018. Diagenetic alterations of Meriones incisors (Rodentia) of El Harhoura 2 cave, Morocco (late Pleistocene–middle Holocene). Paläontol. Z. 92, 163–177.

DeSantis, L.R., Scott, J.R., Schubert, B.W., Donohue, S.L., McCray, B.M., Van Stolk, C.A., Winburn, A.A., Greshko, M.A., O'Hara, M.C., 2013. Direct comparisons of 2D and 3D dental microwear proxies in extant herbivorous and carnivorous mammals. PLoS One 8, e71428.

Dunnett, C.W., 1980. Pairwise multiple comparisons in the unequal variance case. J. Am. Stat. Assoc. 75, 796–800.

Fortelius, M., Solounias, N., 2000. Functional characterization of ungulate molars using the abrasion-attrition wear gradient: a new method for reconstructing paleodiets. Am. Mus. Novit. 3301, 1–36.

Fraser, D., Theodor, J.M., 2011. Comparing ungulate dietary proxies using discriminant function analysis. J. Morphol. 272, 1513–1526.

Gordon, K.D., 1983. Taphonomy of dental microwear: can fossil microwear be studied productively?. Am. J. Phys. Anthropol. 60, 200.

Gordon, K.D., 1984. Taphonomy of dental microwear, II. Am. J. Phys. Anthropol. 64, 164–165.

Happold, D., 2013. Mammals of Africa Volume III. Bloomsbury, London.

Hillson, S., 2005. Teeth, second edition Cambridge University Press, Cambridge.

Kaiser, T.M., Solounias, N., Fortelius, M., Bernor, R.L., Schrenk, F., 2000. Tooth mesowear analysis on Hippotherium primigenium from the Vallesian Dinotheriensande (Germany)-a blind test study. Carolinea. 58, 103–114.

King, T., Andrews, P., Boz, B., 1999. Effect of Taphonomic Processes on Dental Microwear. Am. J. Phys. Anthropol. 108, 359–373.

Kubo, M.O., Yamada, E., Kubo, T., Kohno, N., 2017. Dental microwear texture analysis of extant sika deer with considerations on inter-microscope variability and surface preparation protocols. Biosurf. Biotribol. https://doi.org/10.1016/j.bsbt.2017.11.006.

Mainland, I.L., 2003. Dental microwear in grazing and browsing Gotland sheep (Ovis aries) and its implications for dietary reconstruction. J. Archaeol. Sci. 30, 1513–1527.

Mainland, I.L., 2003. Dental microwear in modern Greek ovicaprids: identifying microwear signatures associated with a diet of leafy hay. Brit. Sch. Athens Stud. 9, 45–50.

Martínez, L.M., Pérez-Pérez, A., 2004. Post-mortem wear as indicator of taphonomic processes affecting enamel surfaces of hominin teeth from Laetoli and Olduvai (Tanzania): implications to dietary interpretations. Anthropology XLII/I, 37–42.

Merceron, G., Schulz, E., Kordos, L., Kaiser, T.M., 2007. Palaeoenvironment of Dryopithecus brancoi at Rudabánya, Hungary: evidence from dental meso- and microwear analyses of large herbivorous mammals. J. Hum. Evol. 53, 331–349.

Purnell, M.A., Darras, P.G., 2016. 3D tooth microwear texture analysis in fishes as a test of dietary hypotheses of durophagy. Surf. Topog. Metrolog. Proper. 4, 014006.

Purnell, M.A., Crumpton, N., Gill, P.G., Jones, G., Rayfield, E.J., 2013. Within-guild dietary discrimination from 3-D textural analysis of tooth microwear in insectivorous mammals. J. Zool. 291, 249–257.

Purnell, M.A., Goodall, R.H., Thomson, S., Matthews, C.J.D., 2017. Tooth microwear texture in odontocete whales: variation with tooth characteristics and implications for dietary analysis. Biosurf. Biotribol. https://doi.org/10.1016/j.bsbt.2017.11.004.

Rensberger, J.M., 1973. An occlusion model for mastication and dental wear in herbivorous mammals. J. Paleontol. 47, 515–528.

Schulz, E., Calandra, I., Kaiser, T.M., 2010. Applying tribology to teeth of hoofed mammals. Scanning 32, 162–182.

Schulz, E., Calandra, I., Kaiser, T.M., 2013. Feeding ecology and chewing mechanics in hoofed mammals: 3D tribology of enamel wear. Wear 300, 169–179.

Schulz, E., Piotrowski, V., Clauss, M., Mau, M., Merceron, G., Kaiser, T.M., 2013. Dietary abrasiveness is associated with variability of microwear and dental surface texture in rabbits. PLoS One 8, e56167.

Scott, J.R., 2012. Dental microwear texture analysis of extant African Bovidae. Mammalia 6, 157–174.

Scott, R.S., Bergstrom, T.S., Brown, C.A., Grine, F.E., Teaford, M.F., Walker, A., Ungar, P.S., 2005. Dental microwear texture analysis shows within-species diet variability in fossil hominins. Nature 436, 693–695.

Scott, R.S., Ungar, P.S., Bergstrom, T.S., Brown, C.A., Childs, B.E., Teaford, M.F., Walker, A., 2006. Dental microwear texture analysis: technical considerations. J. Hum. Evol. 51, 339–349.

Semprebon, G., Rivals, F., 2007. Was grass more prevalent in the pronghorn past? An assessment of the dietary adaptations of Miocene to recent Antilocapridae (Mammalia: Artiodactyla). Palaeogeogr. Palaeoclimatol. Palaeoecol. 253, 332–347.

Skinner, J.D., Chimimba, C.T., 2005. The Mammals of the Southern African Sub-Region. Cambridge University Press, Cambridge.

Solounias, N., Teaford, M., Walker, A., 1988. Interpreting the diet of extinct ruminants: the case of a non-browsing giraffid. Paleobiology 14, 287–300.

Teaford, M.F., 1988. Scanning electron microscope diagnosis of wear patterns versus artifacts on fossil teeth. Scanning Microsc. 2, 1167–1175.

Thenius, E., 1989. Handbuch der Zoologie, Vol VIII/56. Walter de Gruyter, Berlin.

Ungar, P.S., Brown, C.A., Bergstrom, T.S., Walkers, A., 2003. Quantification of dental microwear by tandem scanning confocal microscopy and scale-sensitive fractal analyses. Scanning 25, 185–193.

Ungar, P.S., Merceron, G., Scott, R.S., 2007. Dental Microwear Texture Analysis of Varswater Bovids and early Pliocene Paleoenvironments of Langebaanweg, Western Cape Province, South Africa. J. Mamm. Evol. 14, 163. https://doi.org/10.1007/s10914-007-9050-x.

Ungar, P.S., Grine, F.E., Teaford, M.F., 2008. Dental Microwear and Diet of the Plio-Pleistocene Hominin Paranthropus boisei. PLoS One 3 (4), e2044https://doi.org/10.1371/journal.pone.0002044.

Ungar, P.S., Scott, J.R., Curran, S.C., Dunsworth, H.M., Harcourt-Smith, W.E.H., Lehmann, T., Manthi, F.K., McNulty, K.P., 2012. Early Neogene environments in East Africa: evidence from dental microwear of tragulids. Palaeogeogr. Palaeoclimatol. Palaeoecol. 342-343, 84–96.

Walker, A., Hoeck, H.N., Perez, L., 1978. Microwear of mammalian teeth as an indicator of diet. Science 201, 908–910.

Wasserstraßen-und Schifffahrstverwaltung des Bundes, In: http://www.wsd-west.wsv.de/wasserstrassen/verkehrsweg_rhein/technische_daten/index.html.

Welch, B.L., 1938. The significance of the difference between two means when the population variances are unequal. Biometrika 29, 350–362.

Wilcox, R.R., 2003. Applying Contemporary Statistical Techniques. AcademicPress, San Diego.

Wilcox, R.R., 2005. Introduction to Robust Estimation and Hypothesis Testing, second ed. Elsevier Academic Press, Burlington, SanDiego, London.

Winkler, D.E., Schulz, E., Calandra, I., Gailer, J.P., Landwehr, C., Kaiser, T.M., 2013. Indications for a dietary change in the extinct Bovid genus Myotragus (Plio-Holocene, Mallorca, Spain). Geobios 46, 143–150.

Winkler, D.E., Andrianasolo, T.H., Andriamandimbiarsoa, L., Ganzhorn, J.U., Rakotonfranary, S.J., Kaiser, T.M., Schulz-Kornas, E., 2016. Tooth wear patterns in black rats (Rattus rattus) of Madagascar differ more in relation to human impact than to differences in natural habitats. Ecol. Evol. 6, 2205–2215.

Yuen, K.K., 1974. The two-sample trimmed t for unequal population variances. Biometrika 61, 165–170.

UNCORRECTED PROOF

We applied 3D (enamel) surface texture analysis (compare Schulz et al., 2010, 2013a, 2013b; Calandra et al., 2012) and scale-sensitive fractal analysis (SSFA) using parameters after Ungar et al. (2003) and Scott et al. (2006) using MountainsMap Premium v.7.4 software for data evaluation. To test for the impact of imprecision in misalignment of repeated sampling, we performed a nine-time repetition of the same scan for one original and one moulded sample. Percentage variance was below 1% for ~50°% (moulded sample) and ~57% (original sample) of the parameters. For the parameters *Spd*, *S10z*, *S5p*, *S5v*, *Shv*, *mea,* and *madf* a percentage variance above 10°% (Table S1) was found.

Dataset 1 (Table S2), separated after sediment grain size fraction. Here, we used the mean values of step 1 and calculated a mean for each sediment type ($n = 3$ teeth/mean values).

Dataset 2 (Table S3), all nine teeth per taxon were pooled (ignoring the grain size fraction with which it was tumbled during the experiment). Here, we used the mean values of step 1 and averaged these nine values for t_0 and per tumbling interval (Table 1)

For Dataset 1 we only present descriptive statics, because a sample size of n = 3 per species and sediment grain size fraction is not sufficient to draw statistically significant conclusions. However, we discuss visible trends in parameter value development between tumbling intervals. Trends are calculated by the quotient of tumbling time zero (t_0) and the maximum tumbling time (t_{max}) (16 h for *Otomys* sp., 336 for *Equus* sp. and *C. capreolus,* Table S4). If the value for the quotient (index) is above a value of one outside the standard error, the parameter value is increasing and the trend is described as positive. If the quotient (index) value is below one outside the standard error, the trend is described as negative. In case the quotient (index) value is within the standard error, there is no trend in the parameter.

Contrary, at t_{16} for the teeth of the grazer (*Equus* sp.) a higher number of parameters distinguishes them from the teeth of the untreated (pre-tumbled) browser (*C. capreolus*). The values of the surface texture parameters of *Equus* sp. are lower in *medf* than for the browser, even still after 336 h of tumbling (Fig. 10). Flatness (*FLTp, FLTq, FLTt* (exemplary parameter *FLTq* Fig. 10)), volume (*Vmc, Vv, Vvc* (exemplary parameter *Vv* Fig. 10)), *Sa* and the function parameters *Sxp* and *Smc* are almost unaltered after the whole tumbling treatment and higher in *Equus* sp. (Fig. 10, *FLTp, FLTt, Vmc* and *Vvc* in Table S2).

Generally, we observe two different patterns in parameter values when comparing the original, unaltered surface textures with those after the subsequent tumbling intervals. "Stable" parameters are either not significantly altered by the tumbling process or follow a distinct trend with increasing tumbling time (Fig. 11). "Unstable" parameters show pronounced different values after tumbling and/or follow no distinct trend, alternating between increasing and decreasing parameter values over the tumbling intervals (Fig. 12). We find the highest number of stable parameters in the tumbling regimes using the two smaller grain size fractions (51–168 μm, 112–292 μm). Altogether, those parameters that appear to be unstable, in all tumbling regimes, regardless of grain size fraction, describe the extreme height and depth characteristics of the enamel surface (peaks and dales). The peaks are most exposed to the sediment, and therefore vulnerable for alteration through abrasion. However, it needs to be taken into account, that some of these unstable parameters are also prone to measurement inconsistencies in repeated measurement approach (see Table S1). It is clear that observed post-tumbling alteration in parameter values for the parameters *Spd*, *S10z*, *S5p*, *S5v*, *Shv*, *mea*, and *madf* result from experimental abrasion or are due to the repeated measurement error. However, in all other 44 parameters, the error due to repeated measurements is lower than 5%. Changes in these parameters are therefore considered to be the result of the experimental abrasion.

UNCORRECTED PROOF